

# Boundary effects on the local density of states of one-dimensional Mott insulators and charge density wave states

Dirk Schuricht,<sup>1,2</sup> Fabian H. L. Essler,<sup>3</sup> Akbar Jaefari,<sup>4</sup> and Eduardo Fradkin<sup>4</sup>

<sup>1</sup>*Institute for Theory of Statistical Physics, RWTH Aachen, 52056 Aachen, Germany*

<sup>2</sup>*JARA-Fundamentals of Future Information Technology*

<sup>3</sup>*The Rudolf Peierls Centre for Theoretical Physics,*

*University of Oxford, 1 Keble Road, OX1 3NP, Oxford, UK*

<sup>4</sup>*Department of Physics, University of Illinois at Urbana-Champaign,  
1110 W. Green St, Urbana, Illinois 61801-3080, USA*

(Dated: April 15, 2019)

We determine the local density of states (LDOS) for spin-gapped one-dimensional charge density wave (CDW) states and Mott insulators in the presence of a hard-wall boundary. We calculate the boundary contribution to the single-particle Green function in the low-energy limit using field theory techniques and analyze it in terms of its Fourier transform in both time and space. The boundary LDOS in the CDW case exhibits a singularity at momentum  $2k_F$ , which is indicative of the pinning of the CDW order at the impurity. We further observe several dispersing features at frequencies above the spin gap, which provide a characteristic signature of spin-charge separation. This demonstrates that the boundary LDOS can be used to infer properties of the underlying *bulk* system. In presence of a boundary magnetic field mid-gap states localized at the boundary emerge. We investigate the signature of such bound states in the LDOS. We discuss implications of our results on STM experiments on quasi-1D systems such as two-leg ladder materials like  $\text{Sr}_{14}\text{Cu}_{24}\text{O}_{41}$ . By exchanging the roles of charge and spin sectors, all our results directly carry over to the case of one-dimensional Mott insulators.

## I. INTRODUCTION

Scanning tunneling microscopy (STM) and spectroscopy (STS) methods have proved to be a useful tool for studying strongly correlated electron systems such as carbon nanotubes<sup>1</sup>, high temperature superconductors (HTSC)<sup>2–5</sup> and rare-earth compounds<sup>6</sup>. STM experiments measure the tunneling current  $I$  between the sample and the STM tip as a function of its position  $x$  and the applied voltage  $V$ . This current can be expressed in terms of the local densities of states (LDOS) in the sample  $N(E, x)$  and the tip  $N_{\text{tip}}(E)$  as<sup>5</sup>

$$I(V, x) \propto \int dE [f(E - eV) - f(E)] N_{\text{tip}}(E - eV) N(E, x), \quad (1)$$

where  $f(E)$  denotes the Fermi function. Assuming a structureless density of states in the tip,  $N_{\text{tip}} = \text{const}$ , this gives the following expression for the local tunneling conductance

$$\frac{dI(V, x)}{dV} \propto \int dE f'(E - eV) N(E, x). \quad (2)$$

Eq. (2) shows that the tunneling conductance is proportional to the thermally smeared  $N(E, x)$  of the sample at the position of the tip. A non-trivial spatial dependence of the LDOS arises in presence of impurities. These break translational invariance and lead to a modification of the LDOS in their vicinity, from which one can infer characteristic properties of the *bulk* state of matter as well as the nature of its electronic excitations. Spatial modulations of the LDOS can be analyzed in terms the Fourier transform of the tunneling conductance. It follows from (2) that this quantity is directly proportional to the corresponding Fourier transform of the LDOS,  $N(E, Q)$ . This method of analyzing STM data was used very successfully<sup>3</sup> to study quasiparticle interference in  $\text{Bi}_2\text{Sr}_2\text{CaCu}_2\text{O}_{8+\delta}$ . The spin dependence of the LDOS has also been investigated using magnetic tips<sup>7</sup>. Theoretical studies of STS have focused in particular on Luttinger liquids<sup>8,9</sup> and HTSC<sup>9–11</sup>. In the Luttinger liquid case an impurity has the same effects at low energies as a physical boundary<sup>12</sup>, which motivated studies of the LDOS in the vicinity of a chain end. The case of strongly correlated one-dimensional (1D) systems with spin or charge gaps is of considerable interest as well and pertains to quasi 1D charge density wave (CDW) systems<sup>13</sup> and Mott insulators<sup>14,15</sup>, carbon nanotubes<sup>16</sup>, (doped) two-leg ladder materials<sup>17,18</sup>, and the stripe phases of HTSC<sup>19</sup>. As compared to the Luttinger liquid case the presence of an interaction-induced gap makes these problems much more difficult to treat theoretically. In the following we will determine the LDOS for the low-energy limit of 1D CDW states and Mott insulators in presence of a single boundary. The latter can be thought of as arising as the result of the presence of a strong potential impurity. Alternatively one can imagine inducing a boundary in a two tip STM setup, where the first tip is used to induce a boundary by

applying a high voltage and the LDOS is then measured with a second tip. A short summary of our results has appeared previously<sup>20</sup>.

The outline of this paper is as follows: in section II we present the field theory limit of 1D CDW states and Mott insulators in presence of a single boundary. In section III we summarize our results for the single-particle Green function. These are then used to determine the Fourier transform  $N_\sigma(E, Q)$  of the local density of states for hard-wall boundary conditions in section IV. Signatures of spin and charge excitations visible in  $N_\sigma(E, Q)$  are discussed in some detail. The effects of more general boundary conditions, including the formation of boundary bound states, are described in section V. Section VI deals with the effects of finite temperatures and implications of our results for STM experiments are discussed in section VII. The technical details of our calculations are presented in several appendices.

## II. THE MODEL

Our analysis of the LDOS is based on the continuum description of certain 1D CDW states and Mott insulators. The resulting quantum field theory for both cases is known as the U(1) Thirring model<sup>21</sup> (with two “flavors”.) The latter is known to arise as the effective low-energy description of a number of lattice models of spin-1/2 electrons as we discuss next.

### 1. Half-filled repulsive Hubbard model<sup>22</sup>:

This is the standard model for single band 1D Mott insulators. The Hamiltonian is of the form

$$H = -t \sum_{j,\sigma} \left[ c_{j,\sigma}^\dagger c_{j+1,\sigma} + c_{j+1,\sigma}^\dagger c_{j,\sigma} \right] + U \sum_j \left( n_{j,\uparrow} - \frac{1}{2} \right) \left( n_{j,\downarrow} - \frac{1}{2} \right), \quad (3)$$

where  $n_{j,\sigma} = c_{j,\sigma}^\dagger c_{j,\sigma}$  and  $n_j = n_{j,\uparrow} + n_{j,\downarrow}$  are electron number operators and  $U > 0$ .

### 2. 1D Holstein model<sup>23</sup>:

The Holstein model provides an example of an incommensurate CDW state and describes a partially filled band of spin-1/2 electrons coupled to dispersionless phonons of frequency  $\omega_0 = \sqrt{\frac{k}{M}}$

$$H = -t \sum_{j,\sigma} \left[ c_{j,\sigma}^\dagger c_{j+1,\sigma} + c_{j+1,\sigma}^\dagger c_{j,\sigma} \right] + \sum_j \left[ \frac{P_j^2}{2M} + \frac{k}{2} Q_j^2 \right] - \lambda \sum_{j,\sigma} Q_j n_{j,\sigma}. \quad (4)$$

Integrating out the phonons induces a retarded attractive electron-electron interaction. In the limit  $t \ll \omega_0$  the retardation effects can be neglected, leading to an effective *attractive* Hubbard model with  $U \propto -\lambda^2$ .

### 3. Su-Schrieffer-Heeger model<sup>24</sup>:

A second example of an incommensurate CDW state is provided by the Su-Schrieffer-Heeger model, which describes a partially filled band of spin-1/2 electrons coupled to dispersing phonons

$$H = - \sum_{j,\sigma} \left[ t - \lambda(Q_{j+1} - Q_j) \right] \left[ c_{j,\sigma}^\dagger c_{j+1,\sigma} + c_{j+1,\sigma}^\dagger c_{j,\sigma} \right] + \sum_j \left[ \frac{P_j^2}{2M} + \frac{k}{2} [Q_{j+1} - Q_j]^2 \right]. \quad (5)$$

Taking the continuum limit of (5) (which describes the behavior at low frequencies  $\omega \lesssim t$ ) it was shown by Fradkin and Hirsch<sup>25</sup> that the regime of large phonon frequencies  $t \ll \omega_0 = \sqrt{\frac{k}{M}}$  is described by the U(1) Thirring model<sup>21,26</sup>.

In all three cases a continuum description of the low-energy electronic degrees of freedom is obtained by considering only the modes in the vicinity of the Fermi points  $\pm k_F$ . The lattice electron annihilation operators are expressed in terms of slowly varying right- and left-moving Fermi fields as

$$\frac{c_{j,\sigma}}{\sqrt{a_0}} \rightarrow \Psi_\sigma(x) = e^{ik_F x} R_\sigma(x) + e^{-ik_F x} L_\sigma(x), \quad (6)$$

where  $a_0$  is the lattice spacing,  $x = ja_0$ , and  $\sigma = \uparrow, \downarrow$  labels the spin. In the bulk the fields  $R_\sigma$  and  $L_\sigma$  are bosonized according to

$$R_\sigma^\dagger(\tau, x) = \frac{\eta_\sigma}{\sqrt{2\pi}} \exp\left(\frac{i}{2}\phi_c(\tau, x)\right) \exp\left(\frac{i}{2}f_\sigma\phi_s(\tau, x)\right), \quad (7)$$

$$L_\sigma^\dagger(\tau, x) = \frac{\eta_\sigma}{\sqrt{2\pi}} \exp\left(-\frac{i}{2}\bar{\phi}_c(\tau, x)\right) \exp\left(-\frac{i}{2}f_\sigma\bar{\phi}_s(\tau, x)\right), \quad (8)$$

where the Klein factors  $\eta_\sigma$  satisfy anticommutation rules  $\{\eta_\sigma, \eta_{\sigma'}\} = 2\delta_{\sigma\sigma'}$  and  $f_\uparrow = 1 = -f_\downarrow$ . The fields  $\phi_a$  and  $\bar{\phi}_a$  are the chiral components of the canonical Bose fields  $\Phi_a$  and their dual fields  $\Theta_a$ ,

$$\Phi_a = \phi_a + \bar{\phi}_a, \quad \Theta_a = \phi_a - \bar{\phi}_a, \quad a = c, s. \quad (9)$$

In the bulk the Hamiltonian density then can be cast in the spin-charge separated form

$$\begin{aligned} \mathcal{H}(x) &= \sum_{a=c,s} \mathcal{H}_a(x), \\ \mathcal{H}_a &= \frac{v_a}{16\pi} \left[ \frac{1}{K_a^2} (\partial_x \Phi_a)^2 + K_a^2 (\partial_x \Theta_a)^2 \right] - \frac{g_a}{(2\pi)^2} \cos \Phi_a, \end{aligned} \quad (10)$$

The charge and spin velocities  $v_{c,s}$ , the Luttinger parameters  $K_{c,s}$  and coupling constants  $g_{c,s}$  are functions of the hopping integrals and interaction strengths defining the underlying microscopic model. The cases discussed above correspond to the following parameter regimes:

### 1. Mott insulators

As a result of repulsive electron-electron interactions we have  $v_c > v_s$  and  $K_c < 1$ . The  $\cos \Phi_c$  perturbation in the charge sector is relevant and opens up a gap. The  $\cos \Phi_s$  interaction in the spin sector is marginally irrelevant and flows to zero under the renormalization group. We therefore neglect it in the following.

### 2. Electron-Phonon Systems

At low energies the electron-phonon coupling induces an attractive electron-electron interaction, which results in  $v_s > v_c$  and  $K_c > 1 > K_s$ . The  $\cos \Phi_c$  term is irrelevant, while  $\cos \Phi_s$  term is relevant (marginally relevant in the spin-SU(2) symmetric case  $K_s = 1$ ) and opens up a gap in the spin sector.

In both cases we end up with a spin-charge separated theory of a gapless Luttinger liquid and a sine-Gordon model.

We now imagine a strong, local potential to be present. It is well known from the work of Kane and Fisher<sup>12</sup> that the coupling to the impurity is *relevant*, leading to a crossover at a characteristic dynamical energy (and temperature) scale called “ $T_K$ ”, below which the system is effectively cut into two disconnected parts, and to a pinning of the CDW. This potential could be due to a strong potential impurity or an STM tip. We model the strong impurity potential by a boundary condition on the continuum electron field

$$\Psi_\sigma(x=0) = 0. \quad (11)$$

An important physical consequence of the pinning of the CDW at the impurity (or boundary) is the development of an *induced static CDW order* in this (effectively) quantum critical system. This induced static CDW order, often referred to<sup>27</sup> as a “Friedel oscillation”, leads to non-dispersive features in the LDOS<sup>9</sup> which can be detected in STM and STS experiments.

Our effective low-energy Hamiltonian in the CDW case (in the case of a Mott insulator the roles of spin and charge sectors are interchanged) then becomes

$$H = \sum_{a=c,s} H_a, \quad (12)$$

$$H_c = \frac{v_c}{16\pi} \int_{-\infty}^0 dx \left[ \frac{1}{K_c^2} (\partial_x \Phi_c)^2 + K_c^2 (\partial_x \Theta_c)^2 \right], \quad (13)$$

$$H_s = \frac{v_s}{16\pi} \int_{-\infty}^0 dx \left[ \frac{1}{K_s^2} (\partial_x \Phi_s)^2 + K_s^2 (\partial_x \Theta_s)^2 \right] - \frac{g_s}{(2\pi)^2} \int_{-\infty}^0 dx \cos \Phi_s, \quad (14)$$

where the Bose fields are subject to the hard-wall boundary conditions (we consider more general boundary conditions in Sec. V)

$$\Phi_{c,s}(x=0) = 0. \quad (15)$$

In Appendix A we argue that a weak potential impurity renormalizes to strong coupling even for moderate attractive interactions, suggesting that this situation too can be modeled in terms of the boundary conditions (15). We note that our starting point (12)–(15) differs from the model considered in Ref. 28, where the impurity couples only to the gapless charge sector.

The charge sector (13) describes gapless collective charge excitations propagating with velocity  $v_c$ , which carry charge  $\mp e$  and are commonly referred to as holons and antiholons respectively. On the other hand, the spin excitations or spinons are described by the sine-Gordon model on the half-line (14), which is known to be integrable for quite general boundary conditions<sup>29,30</sup>. In the regime  $K_s > 1/\sqrt{2}$  the elementary bulk excitations are gapped solitons and antisolitons which correspond to up- and down-spin spinons respectively. For  $K_s < 1/\sqrt{2}$  propagating breather (soliton-antisoliton) bound states occur as well. At the Luther-Emery point (LEP)  $K_s = 1/\sqrt{2}$  the spin sector is equivalent to a free massive Dirac fermion<sup>31</sup>. The exact bulk scattering matrix was first derived by Zamolodchikov<sup>32</sup>; the boundary reflection matrices of solitons and antisolitons<sup>29</sup> and breathers<sup>33</sup> were derived by Ghoshal and Zamolodchikov. We will restrict ourselves to the regime  $K_s \geq 1/\sqrt{2}$  throughout, which implies that no breathers exist.

The lattice models discussed above give rise to the simplest kind of one dimensional CDW state/Mott insulator. More complicated versions arise in strongly correlated two- and three-leg ladder systems<sup>19,34</sup>. In these systems, even though electron interactions are strongly repulsive, a Mott state with a finite (and typically large) spin gap is found for a range of dopings close to half filling. While the precise description of the spin sector for two-leg ladders is considerably more complicated<sup>35</sup>, we expect our calculation to capture important qualitative features.

### III. GREEN FUNCTION

The central object of our study is the time-ordered Green function in Euclidean space,

$$G_{\sigma\sigma'}(\tau, x_1, x_2) = -\langle 0_b | \mathcal{T}_\tau \Psi_\sigma(\tau, x_1) \Psi_{\sigma'}^\dagger(0, x_2) | 0_b \rangle, \quad (16)$$

where  $|0_b\rangle$  is the ground state of (12) in the presence of the boundary and  $\tau = it$  denotes imaginary time. The spin takes the values  $\uparrow$  and  $\downarrow$ . At low energies the linearization around the Fermi points yields the decomposition

$$G_{\sigma\sigma'} = e^{ik_F(x_1-x_2)} G_{\sigma\sigma'}^{RR} + e^{-ik_F(x_1-x_2)} G_{\sigma\sigma'}^{LL} + e^{ik_F(x_1+x_2)} G_{\sigma\sigma'}^{RL} + e^{-ik_F(x_1+x_2)} G_{\sigma\sigma'}^{LR}, \quad (17)$$

where e.g.  $G_{\sigma\sigma'}^{RL} = -\langle 0_b | \mathcal{T}_\tau R_\sigma(\tau, x_1) L_{\sigma'}^\dagger(0, x_2) | 0_b \rangle$ . As we are interested in the LDOS, we ultimately want to set  $x_1 = x_2$ . Below we will calculate the spatial Fourier transform of the LDOS as physical properties can be more easily identified. In momentum space the  $RL$  and  $LR$  contributions occur in a different region ( $Q \approx \pm 2k_F$ ) compared to the  $RR$  and  $LL$  parts ( $Q \approx 0$ ). In absence of a boundary we have  $G_{\sigma\sigma'}^{RL} = G_{\sigma\sigma'}^{LR} = 0$  as the charge parts of these Green functions vanish. In presence of a boundary left and right sectors are coupled and the Fourier transform of the Green function (17) concomitantly acquires a nonzero component at  $Q \approx \pm 2k_F$ , which provides a particularly clean way of investigating boundary effects. For this reason we first focus on the  $2k_F$ -part of the Green function and study the small momentum regime afterwards.

The Green function  $G_{\sigma\sigma'}^{RL}$  factorizes into a product of correlation functions in the spin and charge sectors. The charge part can be determined by standard methods<sup>36–38</sup> (see App. B). On the other hand, the integrability of the sine-Gordon model on the half-line (14) enables us to calculate correlation functions in the spin sector using the boundary state formalism introduced by Ghoshal and Zamolodchikov<sup>29</sup> together with a form-factor expansion<sup>39–44</sup>. As we show in App. C the leading terms of this expansion yield ( $\tau > 0$ ,  $x_1 < x_2$ )

$$G_{\sigma\sigma'}^{RL}(\tau, x_1, x_2) = g_c(\tau, x_1, x_2) g_s(\tau, x_1, x_2), \quad (18)$$

$$g_c(\tau, x_1, x_2) = -\frac{\delta_{\sigma\sigma'}}{2\pi} \frac{1}{(v_c\tau - 2iR)^a} \frac{1}{(v_c\tau + 2iR)^b} \left[ \frac{4x_1x_2}{(v_c\tau - ir)(v_c\tau + ir)} \right]^c, \quad (19)$$

$$g_s(\tau, x_1, x_2) = Z_1 e^{i\frac{\pi}{4}} \left[ \frac{1}{\pi} K_0(\Delta\sqrt{\tau^2 + r^2/v_s^2}) + \int_{-\infty}^{\infty} \frac{d\theta}{2\pi} K(\theta + i\frac{\pi}{2}) e^{\theta/2} e^{2i\frac{\Delta}{v_s} R \sinh \theta} e^{-\Delta\tau \cosh \theta} + \dots \right], \quad (20)$$

where  $g_{c,s}$  are the contributions of the charge and spin sectors respectively. Here  $K_0$  is a modified Bessel function and the center-of-mass coordinates are  $R = (x_1 + x_2)/2 < 0$  and  $r = x_1 - x_2 < 0$ . The normalization constant  $Z_1$  was obtained in Ref. [42]. At the LEP<sup>45</sup> and the SU(2) invariant point the boundary reflection amplitude  $K(\theta)$  is given by

$$K(\theta) = i \tanh \frac{\theta}{2} \quad \text{for } K_s = \frac{1}{\sqrt{2}}, \quad K(\theta) = -\frac{\theta}{\pi^{3/2}} \frac{\Gamma(\frac{i\theta}{\pi}) \Gamma(\frac{3}{4} - \frac{i\theta}{2\pi})}{\Gamma(\frac{5}{4} + \frac{i\theta}{2\pi})} 2^{-\frac{i}{\pi}\theta} \sinh \frac{\theta}{2} \quad \text{for } K_s = 1. \quad (21)$$

The expressions for general values of  $K_s$  can be found in Refs. [29,46,47]. The exponents in the charge sector are related to the Luttinger parameter by

$$a = \frac{1}{8} \left( K_c + \frac{1}{K_c} \right)^2, \quad b = \frac{1}{8} \left( K_c - \frac{1}{K_c} \right)^2, \quad c = \frac{1}{8} \left( \frac{1}{K_c^2} - K_c^2 \right). \quad (22)$$

We stress that (20) is independent of  $\sigma$  and that the dependence on  $K_s$  is through the overall normalization constant  $Z_1$  and the boundary reflection amplitude only. The one-particle contributions of the form-factor expansion are given by the first two terms in (20), while the dots represent corrections involving a higher number of particles in the intermediate state as well as higher-order corrections due to the boundary. We have determined the subleading terms in the spin part of the Green function at the LEP and found their contribution to the LDOS calculated below to be negligible (see Sec. IV C).

After analytic continuation to real times  $\tau \rightarrow it$  the Green function (18) exhibits a light cone effect. The first term in (20) shows oscillating behavior for  $r^2 < (v_s t)^2$  but is damped otherwise. Similarly, the second term is oscillating for  $4R^2 < (v_s t)^2$ . These oscillations are due to the propagation of spinons from  $x_2$  to  $x_1$  either directly or via the boundary. In particular, at late enough times both terms will oscillate. A similar light cone effect was observed<sup>48</sup> in the Ising model with a boundary. On the other hand, the charge part (19) possesses singularities at  $v_c t = \pm r$  and  $v_c t = \pm 2R$  due to the propagation of antiholons.

The small momentum regime of the Fourier transform of the LDOS is obtained from ( $\tau > 0$ ,  $x_1 < x_2$ )

$$\begin{aligned} G_{\sigma\sigma'}^{RR}(\tau, x_1, x_2) &= -\frac{\delta_{\sigma\sigma'}}{2\pi} \frac{1}{(v_c \tau - ir)^a} \frac{1}{(v_c \tau + ir)^b} \left[ \frac{4x_1 x_2}{(v_c \tau - 2iR)(v_c \tau + 2iR)} \right]^c \\ &\times Z_1 \left[ \frac{1}{\pi} \sqrt{\frac{i\tau - r/v_s}{i\tau + r/v_s}} K_{1/2}(\Delta \sqrt{\tau^2 + r^2/v_s^2}) + \int_{-\infty}^{\infty} \frac{d\theta}{2\pi} K(\theta + i\frac{\pi}{2}) e^{2i\frac{\Delta}{v_s} R \sinh \theta} e^{-\Delta \tau \cosh \theta} + \dots \right] \\ &= G_{\sigma\sigma'}^{LL}(\tau, x_2, x_1). \end{aligned} \quad (23)$$

Compared to  $G^{RL}$  the singularity at  $v_c t = 2R$  is much softer whereas the one at  $v_c t = r$  is more pronounced.

#### IV. LOCAL DENSITY OF STATES

The knowledge of the Green function (16) enables us to calculate the LDOS, which is directly related to the tunneling current measured in STM experiments. As was noted in Ref. [9] it is useful to consider the Fourier transform of the LDOS as physical properties can be more easily identified. For example, this technique was used to study quasiparticle interference in high-temperature superconductors<sup>3,4</sup> and rare-earth compounds<sup>6</sup>. We will first consider the boundary condition  $\Psi_\sigma(0) = 0$ , which results in the Green function (18) and hence yields a spin-independent LDOS. More general boundary conditions may lead to a spin-dependent LDOS or even the formation of a boundary bound state. We will discuss this case the next section.

The Fourier transform of the LDOS is given by  $N_\sigma(E, Q) = N_\sigma^>(E, Q) + N_\sigma^<(E, Q)$ , where

$$N_\sigma^>(E, Q) = -\frac{1}{2\pi} \int_{-\infty}^0 dx \int_{-\infty}^{\infty} dt e^{i(Et - Qx)} G_{\sigma\sigma}(\tau > 0, x, x) \Big|_{\tau \rightarrow it + \delta}, \quad (24)$$

$$N_\sigma^<(E, Q) = \frac{1}{2\pi} \int_{-\infty}^0 dx \int_{-\infty}^{\infty} dt e^{i(Et - Qx)} G_{\sigma\sigma}(\tau < 0, x, x) \Big|_{\tau \rightarrow it - \delta}. \quad (25)$$

Here the Green function has been analytically continued to real times and we have take the limit  $x_1 \rightarrow x_2 \equiv x$ . We will focus on the LDOS for positive energies in what follows but note that the LDOS for negative energies can be analyzed analogously. As mentioned before, we will be mainly concerned with the  $2k_F$ -component as it vanishes in the absence of the boundary and hence offers a particularly clean way of investigating boundary effects. For  $Q \approx 2k_F$  only  $G_{\sigma\sigma}^{RL}$  contributes and starting from (18) we arrive at the following expression (see App. D)

$$N_\sigma^>(E, 2k_F + q) = \sum_{i=1}^2 N_i^>(E, 2k_F + q) + \dots, \quad (26)$$

$$\begin{aligned} N_i^>(E, 2k_F + q) &= -\Theta(E - \Delta) \frac{Z_1 e^{-i\frac{\pi}{4}(4c+1)} \Gamma(2c+1)}{8\pi^2 v_c^{a+b-1} \Gamma(a+b+2c)} \\ &\times \int_{-A}^A d\theta \frac{h_i(\theta) u_i^{2c+1}}{(E - \Delta \cosh \theta)^{2-a-b}} F_1(2c+1, a, b, a+b+2c; u_i^*, -u_i). \end{aligned} \quad (27)$$

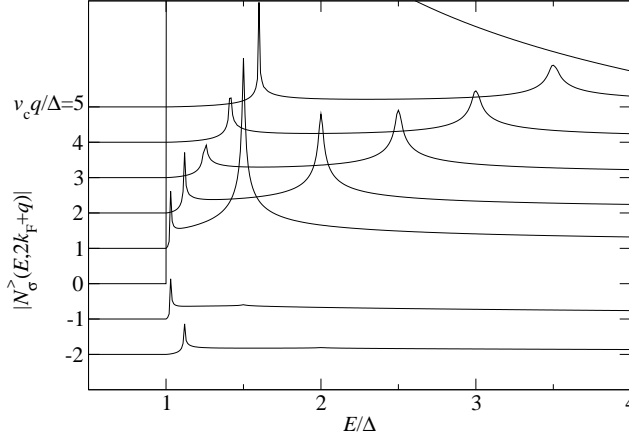


FIG. 1:  $|N_\sigma^>(E, 2k_F + q)|$  (arbitrary units) for  $K_c = 0.8$ ,  $K_s = 1$  and  $v_c = 2v_s$ . The curves are constant  $q$ -scans which have been offset along the y-axis by a constant with respect to one another. The LDOS is dominated by a strong peak at  $q = 0$ , i.e.  $Q = 2k_F$ . We further observe dispersing features at  $E_c = v_c|q|/2 + \Delta$  and  $E_s = \sqrt{(v_s q/2)^2 + \Delta^2}$ . For  $q < 0$  the dispersing features are strongly suppressed.

Here  $|q| \ll 2k_F$ ,  $A = \text{arcosh}(\frac{E}{\Delta})$ ,  $F_1$  denotes Appell's hypergeometric function<sup>49</sup> (see App. E),  $h_1(\theta) = 1$ ,  $h_2(\theta) = K(\theta + i\frac{\pi}{2})e^{\theta/2}$ , and

$$u_1 = \frac{2}{v_c q} (E - \Delta \cosh \theta) + i \text{sgn}\left(\frac{v_s q}{\Delta}\right) \delta, \quad u_2 = \frac{2v_s}{v_c} \frac{E - \Delta \cosh \theta}{v_s q - 2\Delta \sinh \theta} + i \text{sgn}\left(\frac{v_s q}{\Delta} - 2 \sinh \theta\right) \delta, \quad (28)$$

where  $\delta \rightarrow 0+$ . The result (27) is valid for  $a + b < 2$  and  $-1/2 < c$ . Below we plot  $N_\sigma^>(E, 2k_F + q)$  for two different parameter regimes. We smear out singularities by taking  $\delta$  small but finite ( $\delta = 0.01$  unless stated), which mimics broadening by instrumental resolution and temperature in experiments. The results presented below apply to the regime  $T \ll E, \Delta, v_c/a_0$  ( $a_0$  is the lattice spacing), where temperature effects are negligible.

### A. Repulsive Case

We first consider the case  $v_s < v_c$ ,  $K_c < 1$ . This can be thought of as providing a simplified model for the LDOS of a two-leg ladder with repulsive electron-electron interactions. The low-energy theory for the ladder is similar in that there is a gapless charge sector and a gapped spin sector, but the full description of the latter is considerably more complicated<sup>35</sup>.

In Figs. 1 and 2 we plot  $N_\sigma^>(E, 2k_F + q)$  for the case of unbroken spin rotational symmetry ( $K_s = 1$ ). The Fourier transform of the LDOS is dominated by a singularity at momentum  $2k_F$  ( $q = 0$ ), which arises from the contribution  $N_1^>$ . For fixed energy and close to the singularity this term behaves as (see App. F)

$$N_1^>(E, 2k_F + q) \sim \left(\frac{1}{v_c q}\right)^\alpha, \quad \alpha = 1 - \frac{K_c^2}{2}, \quad (29)$$

which implies a phase jump of  $\pi\alpha$  as  $q \rightarrow 0\pm$ . This peak is indicative of the CDW order being pinned at the boundary. We note, however, that the peak occurs at finite energies and hence the underlying process is not static. A similar feature can be seen in the Luttinger liquid case<sup>9</sup>, where the singularity as a function of  $q$  is softer ( $\alpha_{LL} = (1 - K_c)/2$ ).

At low energies above the spin gap  $\Delta$  we further observe two dispersing features associated with the collective spin and charge degrees of freedom respectively. These are broadly similar to the *bulk* single-particle spectral function<sup>50,51</sup> and feature (1) a “charge peak” that follows

$$E_c(q) = \frac{v_c|q|}{2} + \Delta \quad (30)$$

and (2) a “spin peak” at position

$$E_s(q) = \sqrt{\left(\frac{v_s q}{2}\right)^2 + \Delta^2}. \quad (31)$$



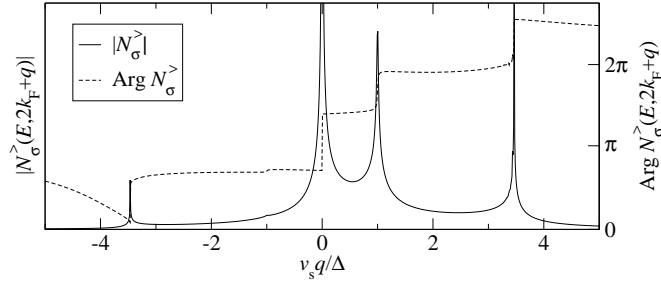


FIG. 2: Constant energy scan for  $E = 2\Delta$ :  $|N_\sigma^>(E, 2k_F + q)|$  (arbitrary units) and  $\text{Arg} N_\sigma^>(E, 2k_F + q)$  for  $K_c = 0.8$ ,  $K_s = 1$  and  $v_c = 2v_s$ . We observe a peak at  $q = 0$  (related to the pinning of the CDW at the boundary) and dispersing features at  $q = \pm 2(E - \Delta)/v_c$  as well as  $q = \pm 2\sqrt{E^2 - \Delta^2}/v_s$ . For  $q < 0$  the dispersing features are strongly suppressed. Furthermore, we observe characteristic jumps in the argument at the positions of the peaks.

We note that neither peak is sharp (i.e. they are not delta-functions) and hence have to be thought of as arising from excitations involving at least two “elementary” constituents. In this way of thinking, the charge peak arises from two-particle excitations composed of a “zero momentum” spinon contributing an energy  $\Delta$  and a gapless antiholon of “momentum”  $q$ . On the other hand, the spin peak can be thought of arising from two-particle excitations composed of a “zero momentum” antiholon and a spinon of “momentum”  $q$ . The appearance of  $v_c/2$  and  $v_s/2$  in (30) and (31), respectively, is due to the fact that the particles have to propagate to the boundary and back, thus covering the distance  $2x$  in time  $t$ . We note that on a technical level the charge peak arises from the contribution  $N_1^>$  to the Fourier transform of the LDOS, whereas the spin peak has its origin in  $N_2^>$ , which encodes the effects of the boundary on the spin degrees of freedom. In the  $q < 0$  region the dispersing features are strongly suppressed and for  $K_c = 1$  the charge feature is found to vanish entirely.

It is instructive to plot  $N_\sigma^>(E, 2k_F + q)$  as a function of  $q$  for fixed energy, see Fig. 2. We observe characteristic jumps in the phase  $\text{Arg} N_\sigma^>$  at the peak positions. This is similar to the Luttinger liquid case<sup>9</sup>.

## B. Attractive case

We now turn to the case of a CDW state arising in a system with (effective) attractive electron-electron interactions. As discussed in the introduction, this case arises in electron-phonon systems. The effective parameters are given by  $v_s > v_c$  and  $K_c > 1 > K_s$ .

In Fig. 3 we plot  $N_\sigma^>(E, 2k_F + q)$  as a function of energy for several values of  $q$  (in units of the spin gap). We again observe a singularity at  $2k_F$ , which arises from (29). The singularity is much less pronounced than in the repulsive case and disappears for  $K_c \geq \sqrt{2}$ . Like in the repulsive case there are several dispersing features:

1. a charge peak at  $E = E_c(q)$ , where  $E_c$  is given by (30);
2. a spin peak at  $E = E_s(q)$ , where  $E_s$  is defined in (31);
3. when  $|q|$  exceeds a critical value  $q_0$  a third dispersing low-energy peak appears (see Fig. 4) at

$$E_{cs}(q) = \frac{v_c|q|}{2} + \Delta \sqrt{1 - \left(\frac{v_c}{v_s}\right)^2} = E_s(q_0) + \frac{v_c}{2}(|q| - q_0), \quad q_0 = \frac{2\Delta v_c}{v_s \sqrt{v_s^2 - v_c^2}}. \quad (32)$$

This feature can be thought of as arising from a “momentum”  $q_0$  spinon and an antiholon carrying “momentum”  $q - q_0$ . We note that in this case the spin and charge excitations have the same group velocity

$$\frac{\partial E_c}{\partial q} = \frac{\partial E_s}{\partial q} \Big|_{q=q_0} = \frac{v_c}{2}. \quad (33)$$

This behavior is reminiscent of what is found for the single-particle spectral function in the bulk<sup>50,51</sup>. The peak splitting and hence the qualitative difference between the repulsive and attractive regime is a consequence of the curvature of the (anti)soliton dispersion relation and hence of the spin gap. In the Luttinger liquid case<sup>9</sup> (where both sectors are massless) there are only two dispersing features in both regimes.

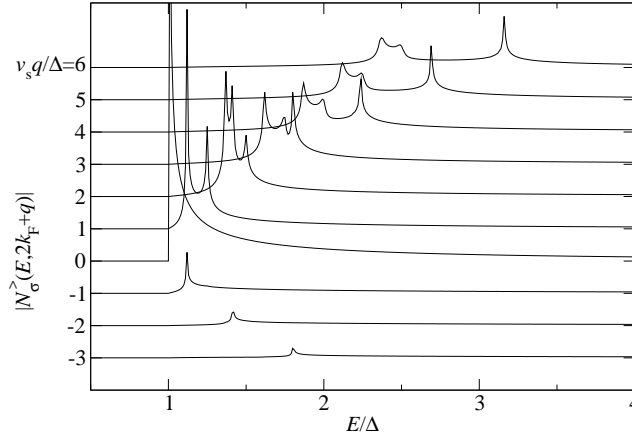


FIG. 3:  $|N_\sigma^>(E, 2k_F + q)|$  (arbitrary units) for  $K_c = 1.2$ ,  $K_s = 1$  and  $v_s = 2v_c$ . The curves are constant  $q$ -scans which have been offset along the y-axis by a constant with respect to one another. The peak at  $q = 0$  is much less pronounced than in the repulsive case (see Fig. 1). We observe dispersing features at  $E_c$ ,  $E_s$ , and  $E_{cs} = v_c|q|/2 + \Delta\sqrt{1 - (v_c/v_s)^2}$  (for  $|q| > q_0$  only).

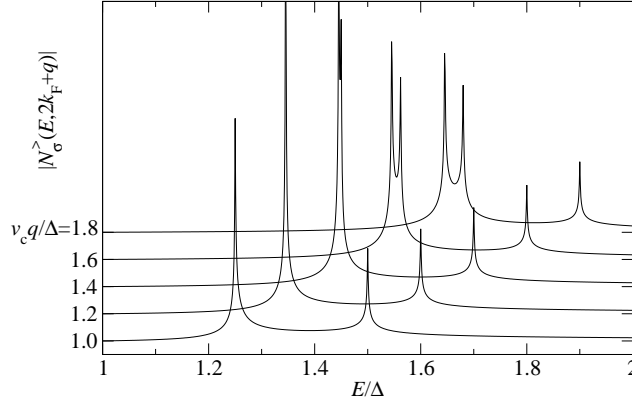


FIG. 4:  $|N_\sigma^>(E, 2k_F + q)|$  (arbitrary units) for  $K_c = 1$ ,  $K_s = 1/\sqrt{2}$ ,  $v_s = 1.5v_c$ ,  $\delta = 0.001$ , and  $v_c q/\Delta = 1.0, \dots, 1.8$ . The curves have been offset along the y-axis by a constant with respect to one another. We observe the splitting of the spin peak at  $E_s$  at the critical momentum  $v_c q_0/\Delta \approx 1.19$ .

### C. Higher-order corrections

As we have indicated in Eq. (20) there are contributions to the LDOS beyond those that we have discussed above. They arise from our calculation of the spin-part of the Green function and are expected to be small<sup>48</sup>. In order to verify that they can indeed be neglected, we have analyzed them in some detail at the LEP  $K_s = 1/\sqrt{2}$ , where the necessary matrix elements take a particularly simple form, which makes the actual calculations much easier.

Our purpose is then to determine further terms in the expansion (26) of  $N_\sigma^>(E, 2k_F + q)$ . We denote by  $N_{nm}$  the contribution to (26) that arises from processes in which  $n$  gapped spinons (which correspond to solitons/antisolitons in the sine-Gordon model describing the spin sector) propagate between  $(0, x_2)$  and  $(\tau, x_1)$ , and which involves the  $m$ 'th power of the boundary reflection matrix  $K$ . The terms discussed above correspond to  $N_{10} = N_1^>$  and  $N_{01} = N_2^>$ . In App. C4 we present some details on the calculation of the terms in the form-factor expansion of  $g_s(\tau, x_1, x_2)$  that give rise to  $N_{nm}$  with  $m + n \leq 3$ . The number of  $\theta$ -integrations in  $N_{nm}$  equals  $m + n$  (cf. (27)). We find that their contributions to the Fourier transform of the LDOS are small. In particular, all qualitative features of the LDOS such as dispersing peaks are already encoded in  $N_{10}$  and  $N_{01}$ . In Fig. 5 we show the leading terms  $N_{10}$  and  $N_{01}$  as well as the sub-leading terms for  $K_c = 1$  and  $v_c > v_s$  for a fixed value of  $q$  as a function of energy. We see that the two leading terms in (26) indeed capture all qualitative features of the LDOS and carry the main part of the spectral weight at low energies  $E \leq 5\Delta$ . The higher-order terms are small compared to  $N_{10}$  and  $N_{01}$ . In particular,  $N_{30}$  vanishes for  $E < 3\Delta$ , since this term originates from a three-particle process. In general, all terms  $N_{nm}$  originating from  $n$ -particle processes vanish for  $E < n\Delta$ . Most importantly, however, the higher-order terms do not possess any singularities. The suppression of subleading terms in the form-factor expansion for bulk two-point functions is a



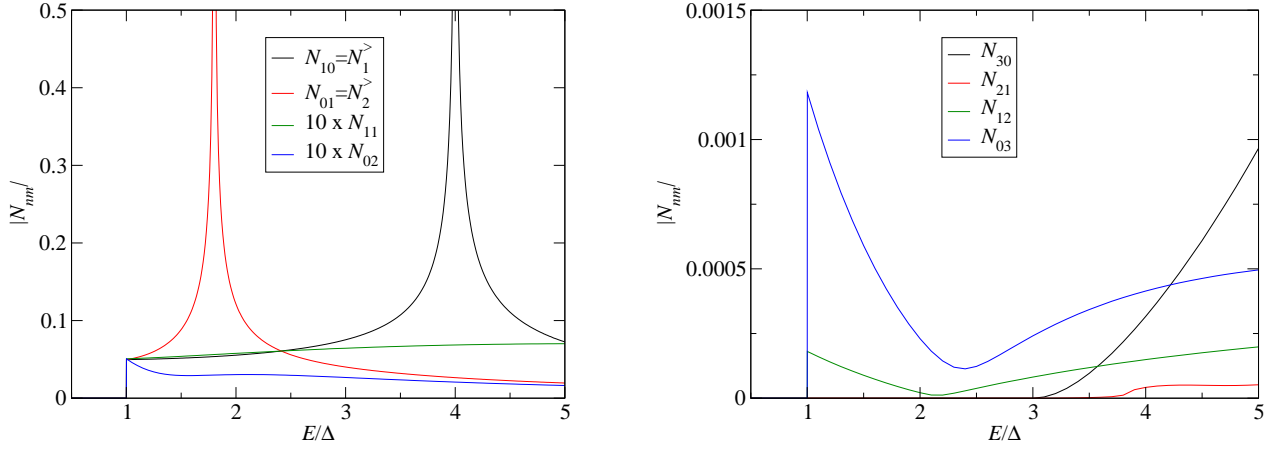


FIG. 5: Left: Comparison of the absolute values of  $N_{10} = N_1^>(E, 2k_F + q)$  and  $N_{01} = N_2^>(E, 2k_F + q)$  to the sub-leading terms  $N_{11}$  and  $N_{02}$  ( $N_{20} = 0$ ). We stress that the scale for the higher-order terms has been magnified. Right: Absolute values of the terms  $N_{30}$ ,  $N_{21}$ ,  $N_{12}$ , and  $N_{03}$ . We stress the different scales on the y-axis. The parameters are  $K_c = 1$ ,  $K_s = 1/\sqrt{2}$ ,  $v_c = 2v_s$ , and  $v_s q/\Delta = 3$ . The three-particle contributions  $N_{30}$  and  $N_{21}$  vanish for  $E < 3\Delta$ . Furthermore, the higher-order terms possess no peaks.

well-known feature of massive theories<sup>44,52,53</sup>, whereas the smallness of terms involving higher powers of the boundary reflection amplitude  $K$  has recently been demonstrated for the Ising model with a boundary magnetic field<sup>48</sup>.

#### D. Small-momentum regime

The small-momentum regime  $Q \approx 0$  of the Fourier transform of the LDOS can be analyzed in the same way as in the  $Q \approx 2k_F$  case discussed above. We note that the LDOS for  $Q \approx 0$  is non-vanishing even in absence of a boundary<sup>50,51</sup>. In the presence of a boundary the Fourier transform of the LDOS for  $Q \approx 0$  is obtained from (23). The leading terms are given by  $N_\sigma^>(E, Q) = \sum_{i=1}^2 N_i^>(E, Q) + \dots$ , where

$$N_i^>(E, Q) = -\Theta(E - \Delta) \frac{Z_1 e^{-i\frac{\pi}{2}(2c+1)} \Gamma(a+b+1)}{4\pi^2 v_c^{a+b-1} \Gamma(2a+2b)} \times \int_{-A}^A d\theta \frac{h_i(\theta) u_i^{2c+1}}{(E - \Delta \cosh \theta)^{2-a-b}} F_1(a+b+1, c, c, 2a+2b; u_i^*, -u_i). \quad (34)$$

Here we have  $|Q| \ll k_F$ ,  $A = \text{arcosh}(\frac{E}{\Delta})$ ,  $h_1(\theta) = e^{\theta/2}$ ,  $h_2(\theta) = K(\theta + i\frac{\pi}{2})$ , and  $u_{1,2}$  are defined in (28) with  $q$  replaced by  $Q$ . The main difference to (26) is the dependence of Appell's hypergeometric function on  $K_c$ .

In Figs. 6 and 7 we plot  $N_\sigma^>(E, Q)$  for the case of repulsive electron interactions and unbroken spin rotational symmetry. It is dominated by a singularity at  $Q = 0$ , which has its origin in  $N_1^>$  and behaves as  $\sim 1/Q$  independently of  $K_c$ . This singularity is more pronounced than its counterpart at  $2k_F$ . We further observe dispersing features at positions  $E_c(Q)$  and  $E_s(Q)$  respectively. Both of these are symmetric under  $Q \rightarrow -Q$ . The peak at  $E_c(Q)$  is strongly suppressed, vanishes for  $K_c = 1$ , and becomes a dip in the attractive regime. The suppression is due to the softness of the singularities of  $G^{RR}$  at  $v_c t = 2R$ . On the other hand, the charge part of (23) has its strongest singularity at  $v_c t = r = 0$ , which results in a background of spectral weight in  $N_\sigma^>(E, Q)$  for all energies above the spin gap.

In the attractive case ( $v_s > v_c$ ) we observe a similar peak-splitting as in the  $2k_F$ -component, but all peaks are very weak.

#### V. GENERAL BOUNDARY CONDITIONS AND BOUNDARY BOUND STATES

So far we have considered the simplest possible boundary conditions corresponding to a spin-independent phase shift of  $\pi$ . Both ways of realizing a boundary in a (quasi) one dimension system that we have discussed above (i.e. as a result of an impurity or in a “two-tip” STS experiment) are expected to give rise to a local potential or magnetic field. These correspond to more general phase shifts for reflection of particles at the boundary. As is well known,

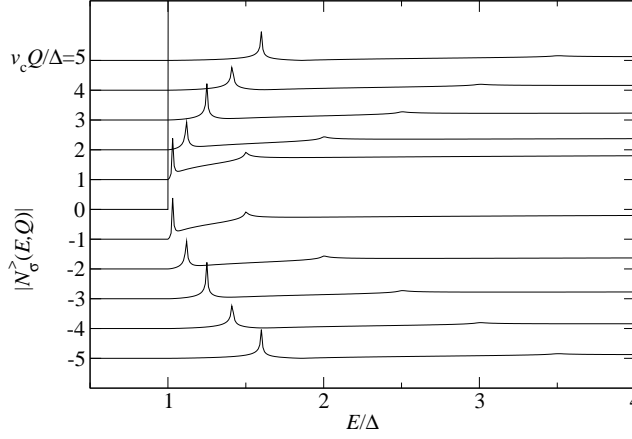


FIG. 6:  $|N_\sigma^>(E, Q)|$  (arbitrary units) for  $K_c = 0.8$ ,  $K_s = 1$  and  $v_c = 2v_s$ . The curves are constant  $Q$ -scans which have been offset along the y-axis by a constant with respect to one another. We observe dispersing features at  $E_c(Q)$  and  $E_s(Q)$ . The charge features are very weak for all momenta. We further observe a constant background at energies larger than the spin gap.

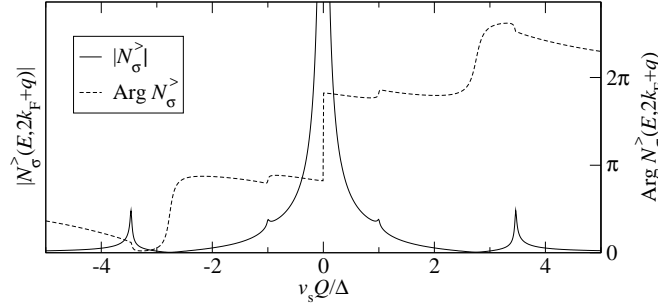


FIG. 7: Constant energy scan for  $E = 2\Delta$ :  $|N_\sigma^>(E, Q)|$  (arbitrary units) and  $\text{Arg} N_\sigma^>(E, Q)$  for  $K_c = 0.8$ ,  $K_s = 1$  and  $v_c = 2v_s$ . We observe a strong peak at  $Q = 0$  and dispersing features at  $Q = \pm 2(E - \Delta)/v_c$  as well as  $Q = \pm 2\sqrt{E^2 - \Delta^2}/v_s$ . Note that  $|N_\sigma^>(E, Q)|$  is symmetric under  $Q \rightarrow -Q$ .

such more general boundary conditions can give rise to boundary bound states, see for example Refs. [54]. These are expected to be visible in the Fourier transform of the LDOS as “resonances” inside the single-particle gap. This is most easily seen by considering a Lehmann representation of  $N_\sigma^>(E, Q)$  in terms of the eigenstates  $|n_b\rangle$  on the half-line

$$N_\sigma^>(E, Q) = \int_{-\infty}^0 dx e^{-iQx} \sum_{n_b} |\langle 0_b | \Psi_\sigma(0, x) | n_b \rangle|^2 \delta(E - E_{n_b}). \quad (35)$$

For boundary bound states  $|bbs, \alpha\rangle$  we have  $0 < E_{bbs, \alpha} < \Delta$ , which leads to features in  $N_\sigma^>(E, Q)$  below the single-particle gap. As we are dealing with a spin-charge separated system, these features will generally not be sharp as the bound state occurs only in the gapped sector of the theory. We now turn to calculating the LDOS in cases where boundary bound states exist. We first consider boundary conditions of the form

$$R_\sigma(\tau, 0) = -e^{-if_\sigma \Phi_s^0/2} L_\sigma(\tau, 0), \quad (36)$$

where  $f_\uparrow = 1 = -f_\downarrow$ . In terms of the Bose fields these boundary conditions read

$$\Phi_c(\tau, 0) = 0, \quad \Phi_s(\tau, 0) = \Phi_s^0, \quad 0 \leq \Phi_s^0 < \pi. \quad (37)$$

We note that these boundary conditions break spin rotational symmetry. However, if we go over to the case of a one-dimensional Mott insulator by exchanging spin and charge degrees of freedom, the spin rotational symmetry remains intact and the boundary conditions correspond to a local potential.

As before we will focus on the  $2k_F$ -component of the Fourier transform of the LDOS. As we have changed the boundary conditions only in the spin sector, the charge part (19) of the chiral Green function remains unchanged.

The two leading terms of the form-factor expansion in the spin sector are still of the form (20), but now the boundary reflection amplitude  $K$  is different and in particular is spin-dependent. At the LEP it is given by<sup>45</sup>

$$K^{\sigma\bar{\sigma}}(\theta) = \frac{\sin\left(i\frac{\theta}{2} - f_{\sigma}\frac{\Phi_s^0}{2}\right)}{\cos\left(i\frac{\theta}{2} + f_{\sigma}\frac{\Phi_s^0}{2}\right)}, \quad K^{\sigma\sigma}(\theta) = K^{\bar{\sigma}\bar{\sigma}}(\theta) = 0. \quad (38)$$

Here we have introduced the notations  $\uparrow = +$  and  $\downarrow = -$  as well as  $\bar{\sigma} = -$  for  $\sigma = +$  and vice versa. We note that as a result of a different choice of phase for the asymptotic states Eq. (38) differs by a minus sign from Ref. [45] (see also App. C). The expressions for general  $K_s$  can be found in Refs. [29,46,47].

In the limit spin rotationally symmetric case  $K_s = 1$  we have  $K^{+-}(\theta) = K^{-+}(\theta) = K(\theta)$ , where  $K(\theta)$  is given in (21). We stress that the Green function remains diagonal in spin space,  $G_{\sigma\sigma'}^{RL} \propto \delta_{\sigma\sigma'}$ , and that the spin-dependence is entirely due to the boundary reflection matrix  $K^{\sigma\bar{\sigma}}$ . Before presenting the resulting LDOS we discuss the emergence of a boundary bound state in the spin sector<sup>29,46,55</sup>. If we choose the phase-shift  $\Phi_s^0$  in the spin sector such that

$$K_s^2\pi < \Phi_s^0, \quad (39)$$

the boundary reflection amplitude  $K^{-+}(\theta)$  has a pole in the physical strip  $0 \leq \Im\theta \leq \pi/2$ . This pole corresponds to a boundary bound state with energy

$$E_{\text{bbs}} = \Delta \sin \gamma, \quad \gamma = \frac{\pi - \Phi_s^0}{2 - 2K_s^2}. \quad (40)$$

The physical nature of the bound state has been discussed by Ghoshal and Zamolodchikov<sup>29</sup>. The classical ground state of the sine-Gordon model on the half-line (14) in the entire range  $0 \leq \Phi_s^0 < \pi$  is characterized by the asymptotic behavior  $\Phi_s \rightarrow 0$  as  $x \rightarrow -\infty$ . On the other hand, there exists a second classically stable state satisfying  $\Phi_s \rightarrow 2\pi$  as  $x \rightarrow -\infty$ . When  $\Phi_s^0$  is sufficiently large this state is expected to be stable in the quantum theory as well.

We note that for  $\Phi_s^0 = \pi$  both states are degenerate and (40) vanishes. In the attractive regime of the sine-Gordon model  $K_s < 1/\sqrt{2}$  additional boundary bound states occur, while in the spin rotationally invariant case  $K_s \rightarrow 1$  the condition  $K_s^2\pi < \Phi_s^0 < \pi$  is never satisfied and hence no boundary bound states exist.

When calculating dynamical response functions in the boundary state formalism additional contributions in the form factor expansions occur upon analytical continuation in the rapidity variables. In particular, the pole of the boundary reflection amplitude in the physical strip gives rise to an additional term linear in  $K$  in the form-factor expansion (20). In the case  $\tau > 0$  and  $x_1 < x_2$  it takes the form (see App. C 5)

$$\Theta\left(\Phi_s^0 - K_s^2\pi\right) \delta_{\sigma\downarrow} Z_1 B e^{\frac{i}{2}\gamma} e^{2\frac{\Delta}{v_s} R \cos \gamma} e^{-\Delta\tau \sin \gamma}, \quad (41)$$

where the constant  $B \geq 0$  is related to the residue of  $K^{\mp\pm}(\theta)$  (see (C47)). At the LEP it equals  $B = -2 \cos \Phi_s^0$ . We stress that this additional term appears in the down-spin channel only, since we have assumed  $0 \leq \Phi_s^0 < \pi$ . If we were to consider  $-\pi < \Phi_s^0 \leq 0$ , we would find a term similar to (41) in the up-spin channel only.

The Fourier transform of the LDOS for the boundary conditions (37) can be expanded as before and is expressed as

$$N_{\sigma}^{>}(E, 2k_F + q) = \sum_{i=1}^3 N_{\sigma,i}^{>}(E, 2k_F + q) + \dots \quad (42)$$

Here the first two terms are again of the form (27), where in the second term  $N_{\sigma,2}^{>}$  we need to replace the boundary reflection amplitude  $K(\theta + i\frac{\pi}{2})$  by its spin-dependent counterpart  $K^{\sigma\bar{\sigma}}(\theta + i\frac{\pi}{2})$ . The third term is obtained from (41) and arises as a result of the presence of a boundary bound state. Explicitly it reads

$$N_{\sigma,3}^{>}(E, 2k_F + q) = \Theta\left(\Phi_s^0 - K_s^2\pi\right) \Theta\left(E - E_{\text{bbs}}\right) \delta_{\sigma\downarrow} \frac{Z_1 B}{4\pi} \frac{\Gamma(2c+1)}{\Gamma(a+b+2c)} \frac{i e^{\frac{i}{2}\gamma} e^{-i\pi c}}{v_c^{a+b-1}} \\ \times \frac{\left(\frac{2}{v_c q}(E - E_{\text{bbs}}) + i \operatorname{sgn}\left(\frac{v_s q}{\Delta}\right) \delta\right)^{2c+1}}{(E - E_{\text{bbs}})^{2-a-b}} F_D^{(3)}(2c+1, a, b, 2c, a+b+2c; u_3^*, -u_3, -u_3'). \quad (43)$$

Here  $F_D^{(3)}$  denotes Lauricella's hypergeometric function of three arguments<sup>56</sup> (see App. E) and

$$u_3 = \frac{2}{v_c q}(E - E_{\text{bbs}}) + i \frac{2\Delta}{v_s q} \cos \gamma, \quad u_3' = i \frac{2\Delta}{v_s q} \cos \gamma, \quad (44)$$

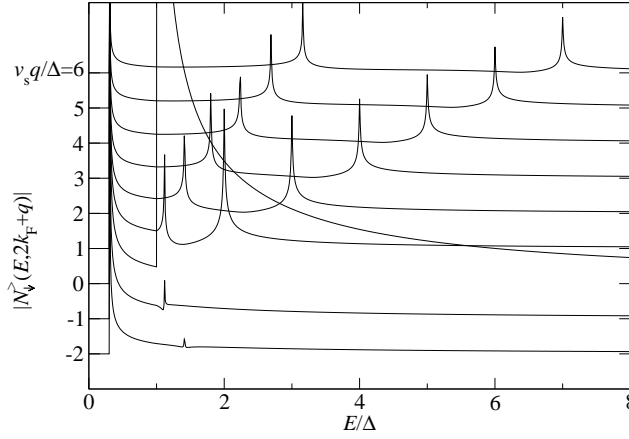


FIG. 8:  $|N_{\downarrow}^>(E, 2k_F + q)|$  (arbitrary units) for  $K_c = 1$ ,  $K_s = 1/\sqrt{2}$ ,  $v_c = 2v_s$ , and  $\Phi_s^0 = 0.9\pi$ . The curves are constant  $q$ -scans which have been offset along the y-axis by a constant with respect to one another. We observe dispersing features at  $E_s(q)$  and  $E_c(q)$  (for  $q > 0$  only) as well as a non-dispersing singularity at  $E = E_{\text{bbs}}$ , which is due to the formation of a boundary bound state in the spin sector.

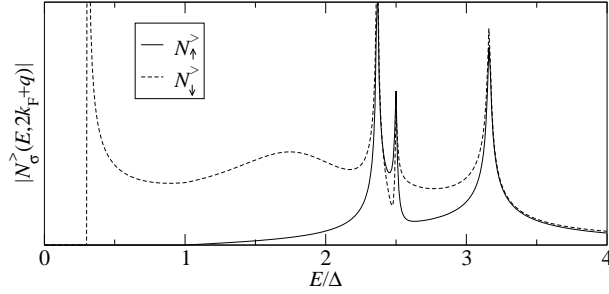


FIG. 9:  $|N_{\uparrow}^>(E, 2k_F + q)|$  (full line) and  $|N_{\downarrow}^>(E, 2k_F + q)|$  (dashed line) for  $v_s q/\Delta = 6$ ,  $K_c = 1$ ,  $K_s = 1/\sqrt{2}$ ,  $v_s = 2v_c$ , and  $\Phi_s^0 = 0.9\pi$ . The broad maximum at  $E \approx 1.8$  is caused by the excitation of the boundary bound state and additional charge excitations.

where the constant  $\gamma$  defined in (40). The Fourier transform of the LDOS (42) has a non-dispersing singularity at its lower threshold

$$N_{\sigma,3}^>(E, 2k_F + q) \propto \frac{\delta_{\sigma\downarrow}}{(E - E_{\text{bbs}})^\alpha}, \quad \alpha = 1 - \frac{1}{2K_c^2}. \quad (45)$$

The emergence of a non-dispersing feature within the spin gap signals the presence of a boundary bound state. In Fourier space the LDOS is a convolution of contributions from the spin and charge sectors. As we are dealing with a bound state in the spin sector, the exponent of the singularity depends only on the Luttinger parameter in the charge sector. We note that the singularity occurs only in the down-spin channel and disappears for  $K_c^2 \leq 1/2$ . On the other hand, in  $N_{\sigma}^<$  the additional feature due to the boundary bound state appears only in the up-spin channel.

In Fig. 8 we plot the down-spin component of (42) for  $v_c > v_s$  as a function of energy for several values of  $q$ . As before, at low energies above the spin gap  $\Delta$  we observe two dispersing features associated with the collective spin and charge degrees of freedom that follow  $E_s$  and  $E_c$  respectively. In addition, we observe the non-dispersing singularity (45) at  $E = E_{\text{bbs}}$ .

In Fig. 9 we plot  $N_{\uparrow}^>$  and  $N_{\downarrow}^>$  as functions of energy for  $v_c < v_s$ . We see that the singularity arising due to the presence of a boundary bound state appears only in the down-spin channel. For either spin polarization we observe three dispersing features at  $E_c(q)$ ,  $E_s(q)$  and  $E_{\text{cs}}(q)$  respectively. Their interpretations are completely analogous to discussion in Sec. IV B. In addition to these sharp peaks we observe a broad maximum in the down-spin channel at energies  $E \approx E_{\text{bbs}} + v_c q/2$ . This feature is suppressed for  $v_c > v_s$ , see Fig. 8. Its physical origin is the simultaneous excitation of the boundary bound state and a finite energy excitation in the charge sector. We note that the asymmetry in  $N_{\uparrow}^>(E, Q) - N_{\downarrow}^>(E, Q)$  could in principle be detected in experiments using a magnetic STM tip. So far we have considered only hard-wall boundary conditions in the charge sector, i.e.  $\Phi_c(x=0) = 0$ . Our analysis can be straightforwardly extended to the case  $\Phi_c(x=0) = \Phi_c^0$ , which in terms of the original electrons corresponds to a local

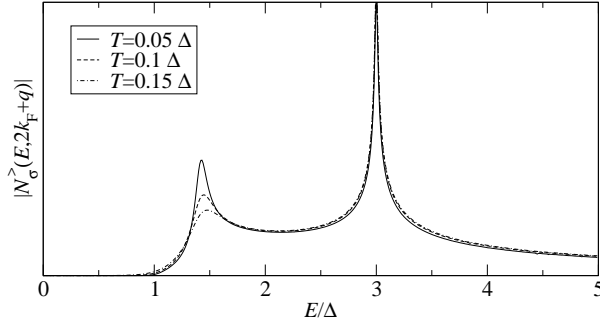


FIG. 10:  $|N_\sigma^>(E, 2k_F + q)|$  (arbitrary units) for  $v_s q/\Delta = 2$ ,  $K_c = K_s = 1$ , and  $v_c = 2v_s$ . We observe spectral weight within the spin gap and a broadening of the propagating peaks, which is much stronger for the spin peak at  $E_s = \sqrt{(\frac{v_s q}{2})^2 + \Delta^2}$ .

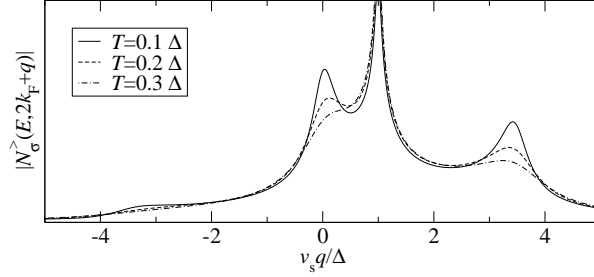


FIG. 11: Constant energy scan of  $|N_\sigma^>(E, 2k_F + q)|$  (arbitrary units) for  $E = 2\Delta$ ,  $K_c = K_s = 1$ , and  $v_c = 2v_s$ . We observe a suppression of the peak at  $q = 0$  related to the pinned CDW.

potential close to the boundary.

## VI. FINITE-TEMPERATURE LDOS

Another interesting issue concerns the effects of a finite temperature on the LDOS. The regime  $T \lesssim \Delta/2$  can in principle be analyzed by generalizing the methods recently developed in Refs. [57] to the boundary state formalism. However, in order to keep matters simple we will restrict ourselves to the regime of very low temperatures  $T \ll \Delta$ . Here the main effects arise from a modification of the dynamical response in the gapless charge sector and correlation functions in the spin sector can be approximated by their  $T = 0$  expressions. This is the case because we only consider response functions that involve both sectors. The charge part of the Green function  $G_{\sigma\sigma'}^{RL}(\tau, x_1, x_2) = g_c(\tau, x_1, x_2) g_s(\tau, x_1, x_2)$  can be evaluated using conformal field theory methods<sup>38,58</sup> and is found to be

$$g_c(\tau, x_1, x_2) = -\frac{\delta_{\sigma\sigma'}}{2\pi} \left( \frac{\pi}{v_c \beta} \right)^{a+b} \frac{1}{\sin^a \left( \frac{\pi}{v_c \beta} (v_c \tau - 2iR) \right)} \frac{1}{\sin^b \left( \frac{\pi}{v_c \beta} (v_c \tau + 2iR) \right)} \times \left[ \frac{\sinh \left( \frac{2\pi}{v_c \beta} x_1 \right) \sinh \left( \frac{2\pi}{v_c \beta} x_2 \right)}{\sin \left( \frac{\pi}{v_c \beta} (v_c \tau - iR) \right) \sin \left( \frac{\pi}{v_c \beta} (v_c \tau + iR) \right)} \right]^c. \quad (46)$$

Here  $\beta = 1/k_B T$  and the exponents in the charge sector were defined in (22). As we have already discussed, the spin part  $g_s(\tau, x_1, x_2)$  is given by (20).

The particle contribution to the Fourier transform of the LDOS is still given by (24). The form-factor expansion in the spin sector results in the series expansion  $N_\sigma^>(E, 2k_F + q) = \sum_i N_i^>(E, 2k_F + q)$ , where the first two terms can be cast in the form

$$N_i^>(E, 2k_F + q) = \frac{Z_1 \pi^{a+b}}{32\pi^5 v_c} \frac{e^{i\frac{\pi}{4}} e^{-i\frac{\pi}{2}(a+b+2c)}}{(v_c \beta)^{a+b-2}} \times \int_{-\infty}^{\infty} d\theta h_i(\theta) \int_{-\infty}^{\infty} dx \int_{-\infty}^x dy \frac{e^{\frac{i\beta}{2\pi}(E_i + \frac{v_c q_i}{2})x}}{\sinh^a(x - i\delta)} \frac{e^{\frac{i\beta}{2\pi}(E_i - \frac{v_c q_i}{2})y}}{\sinh^b(y - i\delta)} \left( \frac{\sinh(\frac{1}{2}(y - x))}{\sinh(\frac{1}{2}(x + y - i\delta))} \right)^{2c}, \quad (47)$$

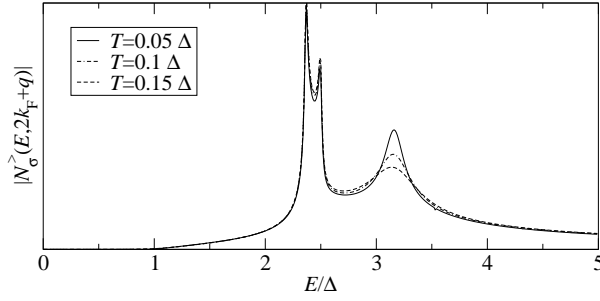


FIG. 12:  $|N_\sigma^>(E, 2k_F + q)|$  (arbitrary units) for  $v_s q/\Delta = 6$ ,  $K_c = K_s = 1$ , and  $v_s = 2v_c$ . We observe again that the broadening of the propagating spin peak is stronger than that of the other peaks.

$$h_1(\theta) = 1, \quad h_2(\theta) = K^{\sigma\bar{\sigma}} (\theta + i\frac{\pi}{2}) e^{\theta/2}, \quad E_1 = E_2 = E - \Delta \cosh \theta, \quad q_1 = q, \quad q_2 = q - \frac{2\Delta}{v_s} \sinh \theta. \quad (48)$$

We have plotted  $N_\sigma^>(E, 2k_F + q)$  for different temperatures in Figs. 10–12. As expected a finite temperature leads to a softening of the spectral gap  $\Delta$ , a suppression of the peak related to the pinned CDW, and a broadening of the dispersing peaks. We observe that the effect of an increasing temperature on the spin peak is much stronger than the effect on the charge peak. The physical reason for this is as follows: In the CDW state only the spin sector is protected by the gap. Thus for  $T \ll \Delta$  there exists a significant number of antiholons in the thermal ground state. They will participate in the distribution of the external momentum  $q$  after the creation of an additional antiholon-spinon pair, thus leading to a decreased probability for the spinon to take the momentum  $q$  and thus to a suppression of the spin peak following  $E_s(q)$ . On the other hand, the charge peak is not affected as the antiholons possess a linear dispersion. This behavior is reminiscent of what is found for the bulk spectral functions<sup>51</sup>.

## VII. IMPLICATIONS FOR STM EXPERIMENTS

STM experiments measure the local tunneling current, which is related to the LDOS by Eq. (1). In particular, the voltage dependence of the tunneling conductance measures the thermally smeared LDOS of the sample at the position of the tip. A possible spin dependence in the LDOS can be detected using a magnetic tip. As we have considered a one-dimensional model, our results apply to quasi-1D materials at energies above the 1D-3D cross-over scale, which is set by the strength of the 3D couplings. Furthermore, the main feature of the model we have studied is the existence of a spectral gap in one of the sectors, while the excitations in the other sector remain gapless. This situation is experimentally realized in various materials, for example in two-leg ladder materials<sup>17</sup>, stripe phases of HTSC<sup>5,9</sup>, carbon nanotubes<sup>1,16</sup>, Bechgaard salts<sup>14</sup>, and chain materials<sup>15</sup> like  $\text{SrCuO}_2$  and  $\text{Sr}_2\text{CuO}_3$ . As our results show, STM experiments can be used to extract rather detailed information regarding bulk excitations by analyzing the modification of the LDOS due to a boundary/impurity.

Perhaps the most interesting materials to which our findings may be applied on a qualitative level are two-leg ladders like<sup>59</sup>  $\text{Sr}_{14}\text{Cu}_{24}\text{O}_{41}$  which possesses a spin gap<sup>60</sup> of  $\Delta \approx 550K$ . The model we have studied captures the most basic features of the low-energy description of (weakly doped) two-leg ladders, namely a gapless charge sector and a gapped spin sector. While the description of the spin sector for weakly doped two-leg ladders is considerably more involved, we expect the gross features to be similar. In particular, we expect peaks to appear in  $N_\sigma(E, Q)$ , which correspond to the pinned CDW order, dispersing spin and charge degrees of freedom, and possibly boundary bound states. We note that our results apply to the regime  $T \ll E, \Delta, v_c/a_0$ , where temperature effects are negligible.

In Ref. [9] it was proposed that STM and STS experiments in HTSC can be used to detect “fluctuating stripes” (i.e. incommensurate spin and charge fluctuations on energy scales small compared to the superconducting gap) by rendering them static by the effects of impurities with a potential comparable to the (low) energy scales of these fluctuations. In that work it was also argued that 1D Luttinger liquids are effectively quantum critical systems and that a form of local (power law) CDW order is effectively induced by impurities (and edges) which pin the phase of the CDW, an effect that we have shown here to take place in a 1D Luther-Emery liquid associated with a CDW. STM and STS experiments in  $\text{Bi}_2\text{Sr}_2\text{CaCu}_2\text{O}_{8+\delta}$  have confirmed the existence of both non-dispersive spectral features in the LDOS associated with “fluctuating stripe order” as well as dispersive features associated with the propagating quasiparticles of the superconductor<sup>2,4,9</sup>. Recent STS experiments in  $\text{Bi}_2\text{Sr}_2\text{CaCu}_2\text{O}_{8+\delta}$  have shown that the dispersive features of the LDOS disappear above the  $T_c$  of the superconductor while the non-dispersive features survive up to the temperature  $T^*$  at which the pseudogap closes<sup>61</sup>.



## VIII. CONCLUSIONS

In this work we have determined the spatial Fourier transform of the LDOS of one-dimensional CDW states and Mott insulators in presence of a boundary. The latter may either model a strong potential impurity or be realized in a two-tip STM experiment. We found that the Fourier transform of the LDOS is dominated by a singularity at an energy equal to the single-particle gap  $\Delta$  and at momentum  $2k_F$ . This feature is indicative of the pinning of the CDW order at the position of the impurity. We observed clear signatures of dispersing spin and charge excitations, which can be used to infer the nature of the underlying electron-electron interactions. In the case of CDW states with repulsive interactions we find a spin mode and a linear dispersing charge mode while for attractive interactions a third dispersing mode appears, which can be thought of as arising from a spin excitation with a fixed momentum  $q_0$  and a charge excitation with momentum  $q - q_0$ .

We have also investigated the modification of the LDOS due to boundary bound states. These may arise in presence of boundary potentials or magnetic fields. We found that boundary bound states give rise to non-dispersing singularities at energies below the single-particle gap. While the bound state is formed in the gapped sector of the theory, the exponent of the corresponding singularity only depends on the Luttinger liquid parameter of the gapless sector. We have analyzed temperature effects in regime  $T \ll \Delta$  and discussed implications of our results for STM measurements on quasi-1D materials such as doped two-leg ladders.

## Acknowledgments

We would like to thank Joe Bhaseen, Dmitry Kovrizhin, and Christian Pfleiderer for useful discussions. DS was supported by the Deutsche Akademie der Naturforscher Leopoldina under grant BMBF-LPD 9901/8-145 while working at the Rudolf Peierls Centre for Theoretical Physics, University of Oxford. This work was also supported by the EPSRC under grant EP/D050952/1 (FHLE), the NSF under grant DMR 0758462 at the University of Illinois (EF), the U.S. Department of Energy, Division of Materials Sciences under Award No. DE-FG02-07ER46453 through the Frederick Seitz Materials Research Laboratory of the University of Illinois (EF, AJ) and the ESF network INSTANS.

## Appendix A: Renormalization group analysis of an impurity potential

Let us consider the low-energy theory of a one-dimensional CDW state on the infinite line  $H = H_c + H_s$ , where

$$H_c = \frac{v_c}{16\pi} \int_{-\infty}^{\infty} dx \left[ \frac{1}{K_c^2} (\partial_x \Phi_c)^2 + K_c^2 (\partial_x \Theta_c)^2 \right], \quad (\text{A1})$$

$$H_s = \frac{v_s}{16\pi} \int_{-\infty}^{\infty} dx \left[ \frac{1}{K_s^2} (\partial_x \Phi_s)^2 + K_s^2 (\partial_x \Theta_s)^2 \right] - \frac{g_s}{(2\pi)^2} \int_{-\infty}^{\infty} dx \cos \Phi_s. \quad (\text{A2})$$

We want to study the effect of an impurity potential at position  $x = 0$ , which in bosonized form reads

$$V_{\text{imp}} = \lambda \int_{-\infty}^{\infty} dx \delta(x) \cos\left(\frac{\Phi_c}{2}\right) \cos\left(\frac{\Phi_s}{2}\right). \quad (\text{A3})$$

As the spin sector in the bulk is massive, we have  $\langle \cos(\Phi_s/2) \rangle \neq 0$ , which implies that at low energies we can approximate  $\cos(\Phi_c/2) \cos(\Phi_s/2)$  in (A3) by  $\langle \cos(\Phi_c/2) \rangle \cos(\Phi_s/2) + \cos(\Phi_c/2) \langle \cos(\Phi_s/2) \rangle$ . Thus in the charge sector we get a boundary sine-Gordon model<sup>62</sup>. For  $K_c^2 < 2$  the impurity scattering potential scales to strong coupling. Hence as long as the interactions are not too attractive the field  $\Phi_c$  gets pinned at the boundary,  $\Phi_c(0) = 0$ . This in turn induces an impurity contribution in the gapped spin sector

$$V_{\text{imp},s} = \lambda \left\langle \cos\left(\frac{\Phi_c(0)}{2}\right) \right\rangle \int_{-\infty}^{\infty} dx \delta(x) \cos\left(\frac{\Phi_s}{2}\right). \quad (\text{A4})$$

If one analyzes the bulk and boundary cosine terms in the resulting impurity model (A2) and (A4) simultaneously, the leading order renormalization group equations are given by the scaling dimensions of the perturbing operators

$$\frac{dg_s}{dl} = 2(1 - K_s^2) g_s, \quad \frac{d\lambda}{dl} = \left(1 - \frac{K_s^2}{2}\right) \lambda. \quad (\text{A5})$$

As long as  $K_s^2 > 2/3$  the boundary term grows more rapidly than the bulk term. Assuming that it reaches the strong-coupling regime first leads to the pinning of the spin field  $\Phi_s(0) = 0$ . This cuts the chain in two half-lines and we obtain the model (12)–(15).

## Appendix B: Calculation of the Green function: Charge sector

The Green function (16) factorizes into a product of correlation functions in the spin and charge sectors. For example, using the bosonization identities (7) and (8) the  $2k_F$ -component  $G_{\sigma\sigma'}^{RL}$  can be written as

$$G_{\sigma\sigma'}^{RL}(\tau, x_1, x_2) = -\frac{1}{2\pi} \left\langle e^{-\frac{i}{2}\phi_c(\tau, x_1)} e^{-\frac{i}{2}\bar{\phi}_c(0, x_2)} \right\rangle_c \left\langle e^{-\frac{i}{2}f_{\sigma}\phi_s(\tau, x_1)} e^{-\frac{i}{2}f_{\sigma'}\bar{\phi}_s(0, x_2)} \right\rangle_s. \quad (B1)$$

Both correlation functions have to be determined in the presence of the boundary at  $x = 0$ . The charge part is calculated below using a standard mode expansion<sup>36</sup>, the spin part will be calculated in App. C.

In order to obtain the correlation functions in the charge sector we first bring the Hamiltonian (13) to standard form by rescaling the fields as  $\Phi_c \rightarrow K_c \Phi_c$ ,  $\Theta_c \rightarrow \Theta_c/K_c$ . The charge parts of the operators (7) and (8) then become

$$\exp\left(\pm \frac{i}{2}\phi_c(\tau, x)\right) \rightarrow e^{i\pi s c/4} \exp\left(\pm \frac{i}{2}c\phi_c(z)\right) \exp\left(\pm \frac{i}{2}s\bar{\phi}_c(\bar{z})\right) = e^{-i\pi s c/4} \exp\left(\pm \frac{i}{2}s\bar{\phi}_c(\bar{z})\right) \exp\left(\pm \frac{i}{2}c\phi_c(z)\right), \quad (B2)$$

$$\exp\left(\pm \frac{i}{2}\bar{\phi}_c(\tau, x)\right) \rightarrow e^{i\pi s c/4} \exp\left(\pm \frac{i}{2}s\phi_c(z)\right) \exp\left(\pm \frac{i}{2}c\bar{\phi}_c(\bar{z})\right) = e^{-i\pi s c/4} \exp\left(\pm \frac{i}{2}c\bar{\phi}_c(\bar{z})\right) \exp\left(\pm \frac{i}{2}s\phi_c(z)\right), \quad (B3)$$

where we have already used (B7) and assumed  $-L < x < 0$ . The constants are parameterized via  $s = \sinh \xi_c$  and  $c = \cosh \xi_c$  with  $K_c = e^{\xi_c}$ . The complex coordinates are defined as  $z = v_c \tau - ix$ ,  $\bar{z} = v_c \tau + ix$ . The charge part of the Green function can hence be obtained from the four-point function

$$\left\langle e^{i\beta_1\bar{\phi}_c(\bar{z}_1)} e^{i\alpha_1\phi_c(z_1)} e^{i\alpha_2\phi_c(z_2)} e^{i\beta_2\bar{\phi}_c(\bar{z}_2)} \right\rangle_{\text{UHP}}, \quad (B4)$$

where  $\alpha_{1,2}, \beta_{1,2} \in \mathbb{R}$ ,  $z_1 = v_c \tau - ix_1$  and  $z_2 = -ix_2$  lie in the upper half-plane.

We calculate (B4) from the mode expansions for the chiral fields  $\phi_c$  and  $\bar{\phi}_c$ . These are obtained by first noting that the fields  $\Phi_c$  and  $\Theta_c$  have to satisfy the equations of motion  $v_c \partial_x \Theta_c = -i \partial_\tau \Phi_c$  and  $\partial_\tau \Theta_c = i v_c \partial_x \Phi_c$  as well as the boundary conditions  $\Phi_c(x=0) = \Phi_c(x=-L) = 0$ . The semi-infinite system is obtained by taking  $L \rightarrow \infty$ . This yields the mode expansions

$$\Phi_c(\tau, x) = -\frac{x}{L} \hat{\Pi}_0 + i \sum_{n=1}^{\infty} \frac{\sin \frac{n\pi x}{L}}{\sqrt{n\pi}} \left( b_n e^{-n\pi v_c \tau/L} - b_n^\dagger e^{n\pi v_c \tau/L} \right), \quad (B5)$$

$$\Theta_c(\tau, x) = \hat{\Theta}_0 - i \frac{v_c \tau}{L} \hat{\Pi}_0 + \sum_{n=1}^{\infty} \frac{\cos \frac{n\pi x}{L}}{\sqrt{n\pi}} \left( b_n e^{-n\pi v_c \tau/L} + b_n^\dagger e^{n\pi v_c \tau/L} \right), \quad (B6)$$

where the zero-mode operator  $\hat{\Pi}_0$  has the discrete spectrum  $2\pi m$ ,  $m \in \mathbb{Z}$ , and  $[\hat{\Theta}_0, \hat{\Pi}_0] = 8\pi i$ ,  $[b_m, b_n^\dagger] = 8\pi \delta_{mn}$ . The mode expansions for the chiral fields are easily obtained via  $\phi_c = (\Phi_c + \Theta_c)/2$  and  $\bar{\phi}_c = (\Phi_c - \Theta_c)/2$ . Their commutation relations are

$$[\phi_c(\tau, x), \bar{\phi}_c(\tau, x')] = \begin{cases} 0 & , \quad x = x' = 0, \\ 4\pi i & , \quad x = x' = -L, \\ 2\pi i & , \quad \text{else,} \end{cases} \quad (B7)$$

as well as  $[\phi_c(\tau, x), \phi_c(\tau, x')] = -[\bar{\phi}_c(\tau, x), \bar{\phi}_c(\tau, x')] = 2\pi i \text{sgn}(x - x')$ , where  $\text{sgn}(0) = 0$ . Similar mode expansions were obtained in Refs. [36]. Given the mode expansion it is straightforward to calculate the four-point function (B4). We find

$$\left\langle e^{i\beta_1\bar{\phi}_c(\bar{z}_1)} e^{i\alpha_1\phi_c(z_1)} e^{i\alpha_2\phi_c(z_2)} e^{i\beta_2\bar{\phi}_c(\bar{z}_2)} \right\rangle_{\text{UHP}} = \frac{C \delta_{\alpha_1+\alpha_2, \beta_1+\beta_2} (z_1 - z_2)^{2\alpha_1\alpha_2} (\bar{z}_1 - \bar{z}_2)^{2\beta_1\beta_2}}{(\bar{z}_1 - z_1)^{2\alpha_1\beta_1} (\bar{z}_1 - z_2)^{2\alpha_2\beta_1} (z_1 - \bar{z}_2)^{2\alpha_1\beta_2} (z_2 - \bar{z}_2)^{2\alpha_2\beta_2}}, \quad (B8)$$

where  $C \in \mathbb{R}$  is a constant which we set to one throughout this manuscript. This result implies Eq. (19). The finite-temperature correlation functions are obtained<sup>38,58</sup> by mapping (B8) onto a cylinder of circumference  $v_c/k_B T$ .

## Appendix C: Calculation of the Green function: Spin sector

The calculation of the correlation functions in the spin sector relies on the integrability of the sine-Gordon model on the half-line. We use the boundary state formalism introduced by Ghoshal and Zamolodchikov<sup>29</sup> together with a form-factor expansion based on form factors obtained by Lukyanov and Zamolodchikov<sup>42</sup>. The analogous expansion for the quantum Ising model has been analyzed in Ref. [48]. We will first discuss the general formalism and then derive (20).

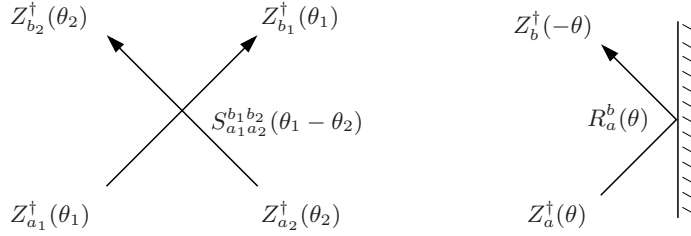


FIG. 13: Two-particle scattering and scattering off the boundary.

### 1. Boundary state formalism and form-factor expansion

Let us consider the sine-Gordon model (14) in the half-plane  $(\tau, x)$ ,  $\tau \in \mathbb{R}$ ,  $-\infty < x \leq 0$ . The boundary is located at  $x = 0$  and  $\tau$  denotes imaginary time ( $\tau = it$ ). The Hilbert space of states associated with the semi-infinite line  $\tau = \text{const}$ ,  $-\infty < x \leq 0$ , is denoted by  $\mathcal{H}_b$ . We obtain the Euclidean action in its standard form by rescaling the fields according to  $\Phi_s \rightarrow \Phi'_s = \Phi_s/K_s$  and  $\Theta_s \rightarrow \Theta'_s = K_s \Theta_s$ . The action of the sine-Gordon model with a boundary is then given by<sup>29</sup> (we set  $v_s = 1$ )

$$\mathcal{S}_{\text{bsG}} = \frac{1}{16\pi} \int d\tau \int_{-\infty}^0 dx \left[ (\partial_\tau \Phi'_s)^2 + (\partial_x \Phi'_s)^2 - \frac{4g_s}{\pi} \cos(K_s \Phi'_s) \right] - g_b \int d\tau \cos \left( \frac{K_s}{2} (\Phi'_s|_{x=0} - \Phi_s^0/K_s) \right), \quad (\text{C1})$$

where  $g_s$ ,  $g_b$  and  $\Phi_s^0$  are free parameters. (We use the conventions  $0 < K_s < 1$ , the action as given in Ref. [29] is obtained by another rescaling of the fields by  $\sqrt{8\pi}$ .) The cases  $g_b = 0$  and  $g_b \rightarrow \infty$  correspond to free and fixed boundary conditions, respectively. We stress that in the case of fixed boundary conditions  $\Phi'_s(x=0) = \Phi_s^0/K_s$  implies  $\Phi_s(x=0) = \Phi_s^0$  in the original system (14). As was conjectured by Ghoshal and Zamolodchikov<sup>29</sup> and shown independently<sup>30</sup> by MacIntyre and Saleur, Skorik and Warner, the classical sine-Gordon model on the half-line (C1) possesses infinitely many integrals of motion and is hence integrable.

We start by summarizing some results for the *bulk* sine-Gordon model, i.e. the theory without boundary. In the repulsive regime ( $K_s > 1/\sqrt{2}$ ) a basis of the Hilbert space  $\mathcal{H}$  is given by scattering states of solitons and antisolitons

$$|\theta_1, \dots, \theta_n\rangle_{a_1, \dots, a_n} = Z_{a_1}^\dagger(\theta_1) \dots Z_{a_n}^\dagger(\theta_n) |0\rangle, \quad {}^{a_n, \dots, a_1} \langle \theta_n, \dots, \theta_1| = \langle 0| Z_{a_n}(\theta_n) \dots Z_{a_1}(\theta_1), \quad (\text{C2})$$

where  $a_i = \pm 1$  and  $|0\rangle$  is the ground state in absence of a boundary. Solitons and antisolitons are created by the operators  $Z_-^\dagger(\theta)$  and  $Z_+^\dagger(\theta)$ . They are characterized by a topological U(1) charge  $-1$  and  $1$ , respectively, while their energy and momentum are parametrized in terms of the rapidity  $\theta$  by  $E = \Delta \cosh \theta$  and  $P = \Delta \sinh \theta$ . The dependence of the soliton mass  $\Delta$  on the bare parameters in the action was obtained in Ref. [64]. We note that in the attractive regime ( $K_s < 1/\sqrt{2}$ ) breather (soliton-antisoliton) bound states occur as well. The operators  $Z_a$  and  $Z_a^\dagger$  fulfill the Faddeev–Zamolodchikov algebra<sup>65</sup> (see Fig. 13)

$$\begin{aligned} Z_{a_1}(\theta_1) Z_{a_2}(\theta_2) &= S_{a_1 a_2}^{b_1 b_2}(\theta_1 - \theta_2) Z_{b_2}(\theta_2) Z_{b_1}(\theta_1), \\ Z_{a_1}^\dagger(\theta_1) Z_{a_2}^\dagger(\theta_2) &= S_{a_1 a_2}^{b_1 b_2}(\theta_1 - \theta_2) Z_{b_2}^\dagger(\theta_2) Z_{b_1}^\dagger(\theta_1), \\ Z_{a_1}(\theta_1) Z_{a_2}^\dagger(\theta_2) &= 2\pi \delta(\theta_1 - \theta_2) \delta_{a_1 a_2} + S_{a_2 b_1}^{b_2 a_1}(\theta_1 - \theta_2) Z_{b_2}^\dagger(\theta_2) Z_{b_1}(\theta_1). \end{aligned} \quad (\text{C3})$$

Here  $S_{a_1 a_2}^{b_1 b_2}(\theta)$  is the two-particle scattering matrix, which was derived in Refs. [32,66]. The unitarity condition reads  $S_{a_1 a_2}^{c_1 c_2}(\theta) S_{c_1 c_2}^{b_1 b_2}(-\theta) = \delta_{a_1}^{b_1} \delta_{a_2}^{b_2}$ . Its non-vanishing elements are

$$S_{++}^{++}(\theta) = S_{--}^{--}(\theta), \quad S_{+-}^{+-}(\theta) = S_{-+}^{+-}(\theta), \quad S_{-+}^{+-}(\theta) = S_{+-}^{+-}(\theta), \quad (\text{C4})$$

for which explicit expressions can be found for example in Ref. [44]. At the LEP ( $K_s = 1/\sqrt{2}$ ) the scattering matrix simplifies to  $S_{a_1 a_2}^{b_1 b_2}(\theta) = -\delta_{a_1}^{b_1} \delta_{a_2}^{b_2}$ , while in the spin symmetric case ( $K_s = 1$ ) one has<sup>46</sup>

$$S_{++}^{++}(\theta) = S_0(\theta) \equiv -\frac{\Gamma(1 + \frac{i\theta}{2\pi}) \Gamma(\frac{1}{2} - \frac{i\theta}{2\pi})}{\Gamma(1 - \frac{i\theta}{2\pi}) \Gamma(\frac{1}{2} + \frac{i\theta}{2\pi})}, \quad S_{+-}^{+-}(\theta) = -\frac{\theta}{\theta - i\pi} S_0(\theta), \quad S_{-+}^{+-}(\theta) = -\frac{i\pi}{\theta - i\pi} S_0(\theta). \quad (\text{C5})$$

We note that the Faddeev–Zamolodchikov algebra (C3) is invariant under the unitary transformation  $Z_a(\theta) \rightarrow e^{i\varphi} Z_a(\theta)$ , which changes the basis of scattering states. In terms of the basis states (C2) the resolution of the identity

reads

$$\text{id} = |0\rangle \langle 0| + \sum_{n=1}^{\infty} \frac{1}{n!} \sum_{\{a_i\}} \int_{-\infty}^{\infty} \frac{d\theta_1 \dots d\theta_n}{(2\pi)^n} |\theta_n, \dots, \theta_1\rangle_{a_n, \dots, a_1}^{a_1, \dots, a_n} \langle \theta_1, \dots, \theta_n|. \quad (\text{C6})$$

The boundary can be introduced<sup>29</sup> as an infinitely heavy, impenetrable particle  $B$  sitting at  $x = 0$ . The ground state in presence of the boundary can then be represented as  $|0_b\rangle = B|0\rangle$ . Scattering of elementary excitations off the boundary is encoded in the relations (see Fig. 13)

$$Z_a^\dagger(\theta)B = R_a^b(\theta)Z_b^\dagger(-\theta)B, \quad (\text{C7})$$

where the functions  $R_a^b(\theta)$  are the single-particle reflection amplitudes. In order to preserve integrability, the boundary reflection matrix  $R(\theta)$  has to satisfy a number of conditions which were discussed in Ref. [29]. At the LEP and for Dirichlet boundary conditions  $\Phi_s(\tau, x=0) = \Phi_s^0$ ,  $0 \leq \Phi_s^0 < \pi$  in the original system (14), it is given by<sup>45</sup>

$$R_\pm^\pm(\theta) = -\frac{\cosh\left(i\frac{\pi}{4} \pm i\frac{\Phi_s^0}{2} + \frac{\theta}{2}\right)}{\cosh\left(i\frac{\pi}{4} \pm i\frac{\Phi_s^0}{2} - \frac{\theta}{2}\right)}, \quad R_\pm^\mp(\theta) = 0. \quad (\text{C8})$$

For  $\pi/2 \leq \Phi_s^0$  the reflection amplitude  $R_\pm^\pm$  possesses a simple pole in the physical strip  $0 \leq \Im \theta \leq \pi/2$ , which indicates the existence of a boundary bound state. The overall sign of the reflection matrix is fixed by the requirement  $-i \text{Res}[R_\pm^\pm(\theta), \theta = \pm i(\Phi_s^0 \mp \pi/2)] = -2 \cos \Phi_s^0 > 0$ , see App. C 5 below. Explicit representations of  $R$  for general  $K_s$  can be found in Refs. [29,46,47]. For  $K_s = 1$  and  $\Phi_s^0 = 0$  one finds in particular

$$R_\pm^\pm(\theta) = -\frac{\Gamma(1 + \frac{i\theta}{2\pi}) \Gamma(\frac{1}{2} - \frac{i\theta}{\pi})}{\sqrt{\pi} \Gamma(1 - \frac{i\theta}{2\pi})} 2^{\pm \frac{\theta}{2}} \left( \cosh \frac{\theta}{2} + i \sinh \frac{\theta}{2} \right), \quad R_\pm^\mp(\theta) = 0. \quad (\text{C9})$$

The vanishing of the off-diagonal amplitudes  $R_\pm^\mp(\theta) = 0$  is a consequence of fixed boundary conditions and holds for general  $K_s$ .

Our aim is to calculate the time-ordered two-point function

$$C(\tau, x_1, x_2) = \langle 0_b | \mathcal{T}_\tau O_1(\tau, x_1) O_2(0, x_2) | 0_b \rangle. \quad (\text{C10})$$

Here the time-dependence of the operators is given by  $O_i(\tau, x) = e^{\tau H_b} O_i(0, x) e^{-\tau H_b}$ , where  $H_b$  is the Hamiltonian of the system in the presence of the boundary (14). Given that in the Euclidean formalism  $\tau$  and  $x$  are interchangeable one may equally well designate  $x$  to be the “Euclidean time”. In this picture the equal-time section is the infinite line,  $x = \text{const}$ ,  $-\infty < \tau < \infty$ , and the associated Hilbert space  $\mathcal{H}$  is that of the corresponding *bulk theory*. The boundary at  $x = 0$  now appears as an initial condition which is expressed in terms of a “boundary state”  $|B\rangle$ . It was shown by Ghoshal and Zamolodchikov<sup>29</sup> that the correlation function (C10) can be expressed as

$$C(\tau, x_1, x_2) = e^{-i\frac{\pi}{2} \sum_i s(O_i)} \frac{\langle 0 | \mathcal{T}_x O_1(\tau, x_1) O_2(0, x_2) | B \rangle}{\langle 0 | B \rangle}. \quad (\text{C11})$$

Here  $s(O_i)$  denotes the Lorentz spin of the operator  $O_i$ ,  $\mathcal{T}_x$  is the  $x$ -ordering operator, which orders the largest  $x_i$  to the right, and  $|0\rangle \in \mathcal{H}$  is the ground state of the model on the infinite line. The spin-dependent phase factor is due to the rotation in Euclidean space; it was for example observed in the Green function of the Ising model with a boundary magnetic field<sup>48</sup>. As we have interchanged space and time and  $x$  is running from 0 to  $-\infty$  in the new framework, the  $\tau$ - and  $x$ -dependence of operators  $O_i(\tau, x)$  is now given by

$$O_i(\tau, x) = e^{-xH} e^{-i\tau P} O_i(0, 0) e^{i\tau P} e^{xH}, \quad (\text{C12})$$

where  $H$  is the Hamiltonian of the system on the infinite line  $-\infty < \tau < \infty$ , and  $P$  is the total momentum.

The boundary state, which encodes all informations on the boundary condition, is given by

$$|B\rangle = \exp\left(\frac{1}{2} \int_{-\infty}^{\infty} \frac{d\xi}{2\pi} K^{ab}(\xi) Z_a^\dagger(-\xi) Z_b^\dagger(\xi)\right) |0\rangle, \quad (\text{C13})$$

where  $K^{ab}(\xi) = R_a^b(i\pi/2 - \xi)$ . For example, the boundary reflection amplitudes  $K$  stated in (21) and (38) are directly obtained from (C8) and (C9). For general  $K_s$  the amplitude  $K^{ab}$  satisfies the boundary cross-unitarity condition<sup>29</sup>

$$K^{ab}(\xi) = S_{cd}^{ab}(2\xi) K^{dc}(-\xi). \quad (\text{C14})$$

Furthermore, for fixed boundary conditions we have  $K^{\pm\pm}(\xi) = 0$ .

Below we calculate the spin part of the Green function (B1) using the boundary formalism presented above. Specifically we will evaluate the correlation function (C11), where the operators  $O_{1,2}$  are the soliton-creating and -annihilating operators  $e^{\pm\frac{i}{2}\phi_s}$  and  $e^{\pm\frac{i}{2}\bar{\phi}_s}$  respectively. We define the  $n$ -particle form factor of an arbitrary operator  $O$  as

$$f_{a_1, \dots, a_n}^O(\theta_1, \dots, \theta_n) = \langle 0 | O | \theta_1, \dots, \theta_n \rangle_{a_1, \dots, a_n} = \langle 0 | O Z_{a_1}^\dagger(\theta_1) \dots Z_{a_n}^\dagger(\theta_n) | 0 \rangle. \quad (C15)$$

The form factors have to satisfy a set of relations, the so-called form-factor axioms<sup>39,41,43</sup>, which we state for completeness in App. C 2. As the operators  $e^{-\frac{i}{2}\phi_s}$  and  $e^{\frac{i}{2}\bar{\phi}_s}$  create one soliton, their respective form factors (C15) vanish unless  $\sum_i a_i = -1$ . The form factors containing up to three particles were derived by Lukyanov and Zamolodchikov<sup>42</sup>. In our conventions the single-particle form factors are given by

$$\langle 0 | e^{-\frac{i}{2}\phi_s} | \theta \rangle_- = \sqrt{Z_1} e^{i\frac{\pi}{8}} e^{\theta/4}, \quad \langle 0 | e^{\frac{i}{2}\bar{\phi}_s} | \theta \rangle_- = \sqrt{Z_1} e^{-i\frac{\pi}{8}} e^{-\theta/4}, \quad (C16)$$

where the normalization constant  $Z_1$  (not to be confused with the Faddeev–Zamolodchikov operators  $Z_\pm(\theta)$  and  $Z_\pm^\dagger(\theta)$ ) depends on  $K_s$  and can be found in Ref. [42]. Evaluation at the LEP yields  $Z_1 \approx 3.32052 \Delta^{5/8}$  whereas at the SU(2) invariant point one finds  $Z_1 \approx 0.921862 \Delta^{1/2}$ . The three-particle form factors are known in terms of contour integrals, which can be explicitly evaluated at the LEP:

$$\left. \begin{aligned} \langle 0 | e^{-\frac{i}{2}\phi_s} | \theta_1, \theta_2, \theta_3 \rangle_{-+-} \\ \langle 0 | e^{\frac{i}{2}\bar{\phi}_s} | \theta_1, \theta_2, \theta_3 \rangle_{--+} \end{aligned} \right\} = -i \sqrt{\frac{Z_1}{2}} e^{\pm i\frac{\pi}{8}} e^{\pm(\theta_1+\theta_2-\theta_3)/4} \frac{\sinh \frac{\theta_1-\theta_2}{2}}{\cosh \frac{\theta_1-\theta_3}{2} \cosh \frac{\theta_2-\theta_3}{2}}. \quad (C17)$$

The three-particle form factors for other orderings of the U(1) indices can be easily obtained using the scattering axiom stated in App. C 2.

The correlation functions to be calculated below contain matrix elements with incoming and outgoing particles,

$${}^{a_1, \dots, a_n} \langle \theta_1, \dots, \theta_n | O | \xi_m, \dots, \xi_1 \rangle_{b_m, \dots, b_1}, \quad (C18)$$

which possess kinematical poles whenever  $\theta_i = \xi_j$  and  $a_i = b_j$ . These matrix elements can be decomposed into a “connected” and “disconnected” contributions. The latter are characterized by the appearance of terms like  $\delta(\theta_i - \xi_j)$ , signaling that some of the particles do not encounter the operator  $O$  in the process described by the matrix element. We deal with these terms following ideas by Smirnov<sup>39</sup> that allow us to analytically continue form factors. Let  $\vec{A} = \{\theta_1, \dots, \theta_n\}$  with  $\theta_1 < \theta_2 < \dots < \theta_n$  and  $\overleftarrow{B} = \{\xi_m, \dots, \xi_1\}$  with  $\xi_m > \xi_{m-1} > \dots > \xi_1$  denote two sets of ordered rapidities and introduce the notations

$$Z[\vec{A}]_{a_1 \dots a_n} \equiv Z_{a_1}(\theta_1) Z_{a_2}(\theta_2) \dots Z_{a_n}(\theta_n), \quad (C19)$$

$$Z^\dagger[\overleftarrow{B}]_{b_m \dots b_1} \equiv Z_{b_m}^\dagger(\xi_m) Z_{b_{m-1}}^\dagger(\xi_{m-1}) \dots Z_{b_1}^\dagger(\xi_1). \quad (C20)$$

Now let  $A_1$  and  $A_2$  be a partition of  $A$ , i.e.  $A = A_1 \cup A_2$ , where  $A_1$  contains  $n(A_1) = n - k$  rapidities. As a consequence of the Faddeev–Zamolodchikov algebra we have

$$Z[\vec{A}]_{a_1 \dots a_n} = S(\vec{A} | \vec{A}_1)_{a_1 \dots a_n}^{c_1 \dots c_n} Z[\vec{A}_2]_{c_1 \dots c_k} Z[\vec{A}_1]_{c_{k+1} \dots c_n}, \quad (C21)$$

where  $S(\vec{A} | \vec{A}_1)$  is the product of two-particle scattering matrices needed to rearrange the order of Faddeev–Zamolodchikov operators in  $Z[\vec{A}]$  to arrive at  $Z[\vec{A}_2]Z[\vec{A}_1]$ . For example, if  $\vec{A} = \{\theta_1, \dots, \theta_4\}$  and  $\vec{A}_1 = \{\theta_2, \theta_3\}$  it is given by

$$S(\vec{A} | \vec{A}_1)_{a_1 \dots a_4}^{c_1 \dots c_4} = \delta_{a_1}^{c_4} S_{a_2 b}^{c_2 c_4}(\theta_2 - \theta_4) S_{a_3 a_4}^{c_3 b}(\theta_3 - \theta_4). \quad (C22)$$

Similarly we have

$$Z^\dagger[\overleftarrow{B}]_{b_m \dots b_1} = Z^\dagger[\overleftarrow{B}_1]_{d_m \dots d_{l+1}} Z^\dagger[\overleftarrow{B}_2]_{d_1 \dots d_l} S(\overleftarrow{B}_1 | \overleftarrow{B})_{b_m \dots b_1}^{d_m \dots d_1}. \quad (C23)$$

Finally we define

$$\delta[\vec{A}, \overleftarrow{B}]_{a_1 \dots a_n}^{b_m \dots b_1} = \delta_{nm} \prod_{j=1}^n 2\pi \delta_{a_j b_j} \delta(\theta_j - \xi_j). \quad (C24)$$

We are now in the position to analytically continue matrix elements as

$$\begin{aligned} \langle 0 | Z[\vec{A}]_{a_1 \dots a_n} O Z^\dagger[\vec{B}]_{b_m \dots b_l} | 0 \rangle &= \sum_{\substack{A=A_1 \cup A_2 \\ B=B_1 \cup B_2}} S(\vec{A}|\vec{A}_1)_{a_1 \dots a_n}^{c_1 \dots c_n} S(\vec{B}|\vec{B}_1)_{b_m \dots b_l}^{d_m \dots d_l} \delta[\vec{A}_2, \vec{B}_2]_{d_l \dots d_1}^{c_1 \dots c_k} \\ &\quad \times \langle 0 | Z[\vec{A}_1 + i0]_{c_{k+1} \dots c_n} O Z^\dagger[\vec{B}_1]_{d_m \dots d_{l+1}} | 0 \rangle. \end{aligned} \quad (C25)$$

Here the sum is over all possible ways to break the sets  $A$  and  $B$  into subsets and  $\vec{A}_1 + i0$  means that all rapidities in  $A_1$  are slightly moved into the upper half-plane. Similarly, we could choose to analytically continue to the lower half-plane

$$\begin{aligned} \langle 0 | Z[\vec{A}]_{a_1 \dots a_n} O Z^\dagger[\vec{B}]_{b_m \dots b_l} | 0 \rangle &= \sum_{\substack{A=A_1 \cup A_2 \\ B=B_1 \cup B_2}} d_{A_2}(O) S(\vec{A}|\vec{A}_2)_{a_1 \dots a_n}^{c_1 \dots c_n} S(\vec{B}|\vec{B}_2)_{b_m \dots b_l}^{d_m \dots d_l} \delta[\vec{A}_2, \vec{B}_2]_{d_l \dots d_1}^{c_1 \dots c_k} \\ &\quad \times \langle 0 | Z[\vec{A}_1 - i0]_{c_{k+1} \dots c_n} O Z^\dagger[\vec{B}_1]_{d_m \dots d_{l+1}} | 0 \rangle. \end{aligned} \quad (C26)$$

The factor  $d_{A_2}(O)$  is due to a possible semi-locality of the operator  $O$  with respect to the fundamental fields creating the excitations<sup>39,41,43,52</sup>. If we use the operators  $O_0^\pm$  defined in (C29) as fundamental fields and denote the mutual semi-locality factor of  $O$  and  $O_0^\pm$  by  $l_\pm(O)$ , it is given by

$$d_A(O) = \prod_{i=1}^{n(A)} l_{a_i}(O) \quad \Rightarrow \quad d_{A_2}\left(e^{-\frac{i}{2}\phi_s}\right) = \prod_{i=1}^k e^{-i\frac{\pi}{2}a_i}, \quad d_{A_2}\left(e^{\frac{i}{2}\bar{\phi}_s}\right) = \prod_{i=1}^k e^{i\frac{\pi}{2}a_i}. \quad (C27)$$

The remaining matrix elements in (C25) and (C26) can be evaluated using crossing

$$\begin{aligned} \langle 0 | Z[\vec{A}_1 \pm i0]_{c_{k+1} \dots c_n} O Z^\dagger[\vec{B}_1]_{d_m \dots d_{l+1}} | 0 \rangle &= {}^{c_{k+1}, \dots, c_n} \langle \theta_{i_{k+1}} \pm i0, \dots, \theta_{i_n} \pm i0 | O | \xi_{j_m}, \dots, \xi_{j_{l+1}} \rangle_{d_m, \dots, d_{l+1}} \\ &= d_{A_1}(O) C_{c_{k+1}e_{k+1}} \dots C_{c_n e_n} f_{e_{k+1}, \dots, e_n, d_m, \dots, d_{l+1}}^O(\theta_{i_{k+1}} + i\pi \pm i\eta_{i_{k+1}}, \dots, \theta_{i_n} + i\pi \pm i\eta_{i_n}, \xi_{j_m}, \dots, \xi_{j_{l+1}}), \end{aligned} \quad (C28)$$

where  $C_{ab} = \delta_{a+b,0}$  is the charge conjugation matrix and  $\eta_i \rightarrow 0+$ . The analytic continuation of general matrix elements (C18) with arbitrary orders of the rapidities can be obtained using the scattering axiom (see below).

## 2. Form-factor axioms

For completeness we state here the used form-factor axioms. We follow Delfino<sup>43</sup>. The  $n$ -particle form factor of an arbitrary operator  $O$  was defined in (C15). We use the local bosonic fields

$$O_0^\pm(\tau, x) = \exp\left(\mp \frac{1}{4K_s} \int_{-\infty}^{\tau} d\tau \partial_x \Phi'_s(\tau, x)\right), \quad (C29)$$

as fundamental fields for the creation of solitons and antisolitons. The corresponding creation and annihilation operators are  $Z_\pm^\dagger(\theta)$  and  $Z_\pm(\theta)$  introduced in (C2). The form-factor axioms read:

1. The form factors  $f_{a_1, \dots, a_n}^O(\theta_1, \dots, \theta_n)$  are meromorphic functions of  $\theta_n$  in the physical strip  $0 \leq \text{Im } \theta_n \leq 2\pi$ . There exist only simple poles in this strip.
2. Scattering axiom:

$$\begin{aligned} f_{a_1, \dots, a_i, a_{i+1}, \dots, a_n}^O(\theta_1, \dots, \theta_i, \theta_{i+1}, \dots, \theta_n) \\ = S_{a_i a_{i+1}}^{b_i b_{i+1}}(\theta_i - \theta_{i+1}) f_{a_1, \dots, b_{i+1}, b_i, \dots, a_n}^O(\theta_1, \dots, \theta_{i+1}, \theta_i, \dots, \theta_n), \end{aligned}$$

with the scattering matrix  $S_{a_i a_{i+1}}^{b_i b_{i+1}}(\theta_i - \theta_{i+1})$ . At the free-fermion point it is given by  $S_{a_1 a_2}^{b_1 b_2}(\theta) = -\delta_{a_1}^{b_1} \delta_{a_2}^{b_2}$ .

3. Periodicity axiom:

$$f_{a_1, \dots, a_n}^O(\theta_1 + 2\pi i, \theta_2, \dots, \theta_n) = l_{a_1}(O) f_{a_2, \dots, a_n, a_1}^O(\theta_2, \dots, \theta_n, \theta_1),$$

where  $l_\pm(O)$  is the mutual semi-locality factor between the operator  $O$  and the fundamental fields  $O_0^\pm$ . In particular, we have  $l_\pm(e^{-\frac{i}{2}\phi_s}) = \mp i$  and  $l_\pm(e^{\frac{i}{2}\bar{\phi}_s}) = \pm i$ .



4. Lorentz transformations:

$$f_{a_1, \dots, a_n}^O(\theta_1 + \Lambda, \dots, \theta_n + \Lambda) = e^{s(O)\Lambda} f_{a_1, \dots, a_n}^O(\theta_1, \dots, \theta_n),$$

where  $s(O)$  denotes the Lorentz spin of  $O$ . Here we have  $s(e^{\pm \frac{1}{2}\phi_s}) = 1/4$  and  $s(e^{\pm \frac{1}{2}\bar{\phi}_s}) = -1/4$ .

5. Annihilation pole axiom:

$$\begin{aligned} & \text{Res}[f_{a,b,a_1, \dots, a_n}^O(\theta', \theta, \theta_1, \dots, \theta_n), \theta' = \theta + i\pi] \\ &= i C_{ac} f_{b_1, \dots, b_n}^O(\theta_1, \dots, \theta_n) \left[ \delta_{a_1}^{b_1} \dots \delta_{a_n}^{b_n} \delta_b^c - l_a(O) S_{c_1 a_1}^c(\theta - \theta_1) S_{c_2 a_2}^{c_1 b_2}(\theta - \theta_2) \dots S_b^{c_{n-1} b_n}(\theta - \theta_n) \right], \end{aligned}$$

with the charge conjugation matrix  $C_{ab} = \delta_{a+b,0}$ . If there do not exist bound states in the model, i.e. for  $K_s^2 \geq 1/2$ , these are the only poles of the form factors.

We note that the precise form of the axioms depends on the basis of scattering states and thus changes under a unitary transformation of the operators  $Z_a(\theta)$ .

### 3. Correlation functions

In this appendix we derive (20) using the boundary state formalism. We start with the spin part of (B1). After the rotation in Euclidean space this is given by (C11). We insert a resolution of the identity (C6) and expand the boundary state (C13) in powers of  $K$ . This yields the double expansion ( $\tau > 0$ ,  $x_1 < x_2$ )

$$\left\langle e^{-\frac{1}{2}f_\sigma \phi_s(\tau, x_1)} e^{-\frac{1}{2}f_{\sigma'} \bar{\phi}_s(0, x_2)} \right\rangle_s = \langle 0 | e^{-\frac{1}{2}f_\sigma \phi_s(\tau, x_1)} e^{-\frac{1}{2}f_{\sigma'} \bar{\phi}_s(0, x_2)} | B \rangle = \delta_{\sigma\sigma'} \sum_{n=0}^{\infty} \sum_{m=0}^{\infty} C_{n, 2m}(\tau, x_1, x_2), \quad (\text{C30})$$

where we have used  $s(e^{\pm \frac{1}{2}\phi_s}) + s(e^{\pm \frac{1}{2}\bar{\phi}_s}) = 0$ . The operators  $e^{\pm \frac{1}{2}\phi_s}$  and  $e^{\pm \frac{1}{2}\bar{\phi}_s}$  change the  $U(1)$  charge by  $\mp 1$  and  $\pm 1$ , respectively. As the boundary state has vanishing  $U(1)$  charge for Dirichlet boundary conditions ( $K^{\sigma\sigma}(\xi) = 0$ ) the correlation function is diagonal in spin space. Furthermore we have defined the auxiliary functions

$$\begin{aligned} C_{n, 2m}(\tau, x_1, x_2) &= \frac{1}{2^m} \frac{1}{m!} \frac{1}{n!} \int_{-\infty}^{\infty} \frac{d\xi_1 \dots d\xi_m}{(2\pi)^m} \int_{-\infty}^{\infty} \frac{d\theta_1 \dots d\theta_n}{(2\pi)^n} K^{a_1 b_1}(\xi_1) \dots K^{a_m b_m}(\xi_m) \\ &\times \langle 0 | e^{-\frac{1}{2}f_\sigma \phi_s(\tau, x_1)} | \theta_n, \dots, \theta_1 \rangle_{c_n, \dots, c_1} {}^{c_1, \dots, c_n} \langle \theta_1, \dots, \theta_n | e^{-\frac{1}{2}f_{\sigma'} \bar{\phi}_s(0, x_2)} | -\xi_1, \xi_1, \dots, -\xi_m, \xi_m \rangle_{a_1, b_1, \dots, a_m, b_m}. \end{aligned} \quad (\text{C31})$$

We use the notations  $\uparrow = +$ ,  $\downarrow = -$ ,  $\bar{\sigma} = -$  for  $\sigma = +$  and vice versa. We label the various terms in the expansion (C30) by the numbers of particles in the intermediate state  $n$  and in the boundary state  $2m$ , respectively. The  $\tau$ - and  $x$ -dependence of the operators is given by (C12). We have already assumed  $x_1 < x_2$  to avoid additional phases due to the mutual semi-locality of the operators. For the calculation of the LDOS we have to take  $x_1 \rightarrow x_2$  finally. The second matrix element possesses kinematical poles which we treat using (C25). This introduces a third, finite summation in (C30), which labels the “connectedness” of the corresponding terms. We note, however, that (C25) and (C26) yield the same results.

Let us start with the first non-vanishing term in the series (C30), which is using (C12) given by (we recall that the center-of-mass coordinates are defined by  $R = (x_1 + x_2)/2 < 0$  and  $r = x_1 - x_2 < 0$ )

$$C_{10} = \int_{-\infty}^{\infty} \frac{d\theta}{2\pi} \langle 0 | e^{-\frac{1}{2}f_\sigma \phi_s} | \theta \rangle_c {}^c \langle \theta | e^{-\frac{1}{2}f_{\sigma'} \bar{\phi}_s} | 0 \rangle e^{\frac{\Delta}{v_s} r \cosh \theta} e^{i\Delta \tau \sinh \theta} = Z_1 e^{i\frac{\pi}{4}} \int_{-\infty}^{\infty} \frac{d\theta}{2\pi} e^{\frac{\Delta}{v_s} r \cosh \theta} e^{i\Delta \tau \sinh \theta}. \quad (\text{C32})$$

We can rewrite this by shifting the contour of integration as  $\theta \rightarrow \theta + i\pi/2$ . The contributions of  $\Re \theta = \pm\infty$  vanish due to the exponential factors. As there are no poles in the strip  $0 \leq \Im \theta \leq \pi/2$  we find

$$C_{10} = Z_1 e^{i\frac{\pi}{4}} \int_{-\infty}^{\infty} \frac{d\theta}{2\pi} e^{i\frac{\Delta}{v_s} r \sinh \theta} e^{-\Delta \tau \cosh \theta} = \frac{Z_1}{\pi} e^{i\frac{\pi}{4}} K_0(\Delta \sqrt{\tau^2 + r^2/v_s^2}), \quad (\text{C33})$$

where  $K_0$  denotes the modified Bessel function<sup>63</sup>.

The first term containing the boundary reflection amplitude  $K$  is  $C_{12}$ . For  $f_\sigma = -1$  it reads

$$C_{12} = \frac{1}{2} \int_{-\infty}^{\infty} \frac{d\xi}{2\pi} \frac{d\theta}{2\pi} K^{ab}(\xi) \langle 0 | e^{\frac{1}{2}\phi_s} | \theta \rangle_c {}^c \langle \theta | e^{\frac{1}{2}\bar{\phi}_s} | -\xi, \xi \rangle_{ab} e^{\frac{\Delta}{v_s} r \cosh \theta} e^{2\frac{\Delta}{v_s} x_2 \cosh \xi} e^{i\Delta \tau \sinh \theta}, \quad (\text{C34})$$

The first form factor vanishes for  $c \neq +$  and can be evaluated using (C28)

$$\langle 0 | e^{\frac{i}{2}\phi_s} | \theta \rangle_+ = {}^+ \langle \theta | e^{-\frac{i}{2}\phi_s} | 0 \rangle^* = e^{i\frac{\pi}{2}} \langle 0 | e^{-\frac{i}{2}\phi_s} | \theta + i\pi \rangle_-^* = \sqrt{Z_1} e^{i\frac{\pi}{8}} e^{\theta/4}. \quad (\text{C35})$$

For the second matrix element we use (C25), which explicitly yields

$$\begin{aligned} {}^+ \langle \theta | e^{\frac{i}{2}\bar{\phi}_s} | -\xi, \xi \rangle_{-+} &= {}^+ \langle \theta + i0 | e^{\frac{i}{2}\bar{\phi}_s} | -\xi, \xi \rangle_{-+} + 2\pi\delta(\theta - \xi) \langle 0 | e^{\frac{i}{2}\bar{\phi}_s} | -\xi \rangle_- + 2\pi\delta(\theta + \xi) S_{-+}^{+-}(-2\xi) \langle 0 | e^{\frac{i}{2}\bar{\phi}_s} | \xi \rangle_- , \\ {}^+ \langle \theta | e^{\frac{i}{2}\bar{\phi}_s} | -\xi, \xi \rangle_{+-} &= {}^+ \langle \theta + i0 | e^{\frac{i}{2}\bar{\phi}_s} | -\xi, \xi \rangle_{+-} + 2\pi\delta(\theta + \xi) S_{+-}^{+-}(-2\xi) \langle 0 | e^{\frac{i}{2}\bar{\phi}_s} | \xi \rangle_- . \end{aligned} \quad (\text{C36})$$

This leads to two contributions which we denote by  $C_{12}^0$  and  $C_{12}^1$  respectively. The additional upper index denotes the number of lines connecting the operators (the “connectedness”), i.e. the number of internal  $\theta$ -integrations left after using (C25). The first terms on the right-hand side of (C36) in each equation together yield  $C_{12}^1$ . We will calculate this term at the LEP in the next section. On the other hand, the disconnected piece is given by

$$C_{12}^0 = \frac{Z_1}{2} \int_{-\infty}^{\infty} \frac{d\xi}{2\pi} \left[ K^{-+}(\xi) + K^{+-}(-\xi) S_{+-}^{+-}(2\xi) + K^{-+}(-\xi) S_{-+}^{+-}(2\xi) \right] e^{\xi/2} e^{2\frac{\Delta}{v_s} R \cosh \xi} e^{i\Delta\tau \sinh \xi}. \quad (\text{C37})$$

Using the boundary cross-unitarity (C14) the terms in the square brackets equal  $2K^{-+}(\xi)$ . With the similar calculation for  $f_\sigma = 1$  we arrive at

$$C_{12}^0 = Z_1 \int_{-\infty}^{\infty} \frac{d\xi}{2\pi} K^{\sigma\bar{\sigma}}(\xi) e^{\xi/2} e^{2\frac{\Delta}{v_s} R \cosh \xi} e^{i\Delta\tau \sinh \xi}, \quad (\text{C38})$$

The second term in (20) is now obtained by shifting the contour of integration as  $\xi \rightarrow \xi + i\pi/2$  while noting that for the boundary condition  $\Phi_s(x=0) = 0$  the reflection amplitude does not depend on  $\sigma$  and is analytic in the physical strip  $0 \leq \text{Im} \xi \leq \pi/2$ . If  $\Phi_s(x=0) \neq 0$ , however, the reflection amplitude may possess a pole in the physical strip. We will calculate the resulting term in App. C 5.

#### 4. Higher-order terms

In order to estimate the truncation error in (20), we will calculate the leading corrections due to a higher number of particles in the intermediate state as well as higher-order corrections due to the boundary. The resulting corrections to the LDOS are discussed in Sec. IV C. We will restrict ourselves to the LEP, where the form factors are given by (C17),  $S_{a_1 a_2}^{b_1 b_2}(\theta) = -\delta_{a_1}^{b_1} \delta_{a_2}^{b_2}$ , and  $K^{ab}(\xi) = -K^{ba}(-\xi)$ .

The leading correction due to a higher number of particles in the intermediate state is given by  $C_{30}$ ,

$$C_{30} = Z_1 \frac{e^{i\frac{\pi}{4}}}{4} \int_{-\infty}^{\infty} \frac{d\theta_1 d\theta_2 d\theta_3}{(2\pi)^3} \frac{\sinh^2 \frac{\theta_1 - \theta_2}{2}}{\cosh^2 \frac{\theta_1 - \theta_3}{2} \cosh^2 \frac{\theta_2 - \theta_3}{2}} e^{i\frac{\Delta}{v_s} r \sum_i \sinh \theta_i} e^{-\Delta\tau \sum_i \cosh \theta_i}. \quad (\text{C39})$$

The resulting contribution to the LDOS discussed in Sec. IV C is denoted by  $N_{30}$ . We note that  $C_{20} = 0$ .

The first sub-leading term due to the boundary is given by  $C_{12}^1$ , i.e. the connected piece of  $C_{12}$  obtained from the first terms in (C36). For  $f_\sigma = -1$  this term reads using (C35) and (C17)

$$C_{12}^1 = Z_1 \frac{e^{-i\frac{\pi}{4}}}{\sqrt{2}} \int_{-\infty}^{\infty} \frac{d\xi d\theta}{2\pi} \frac{K^{-+}(\xi)}{\cosh \xi} \frac{\sinh \frac{\theta + \xi + i\pi}{2}}{\cosh \frac{\theta - \xi + i\pi + i\eta}{2}} e^{\xi/2} e^{i\frac{\Delta}{v_s} r \cosh \theta} e^{2\frac{\Delta}{v_s} x_2 \cosh \xi} e^{i\Delta\tau \sinh \theta}, \quad (\text{C40})$$

where  $\eta \rightarrow 0+$ . We can handle the singularity at  $\theta = \xi - i\eta$  by shifting  $\theta \rightarrow \theta + i\pi/2$ . Performing the same steps for  $f_\sigma = 1$  we arrive at

$$C_{12}^1 = Z_1 \frac{e^{-i\frac{\pi}{4}}}{\sqrt{2}} \int_{-\infty}^{\infty} \frac{d\xi d\theta}{2\pi} \frac{K^{\sigma\bar{\sigma}}(\xi)}{\cosh \xi} \frac{e^{\xi+\theta} - i}{i e^{\xi} + e^{\theta}} e^{\xi/2} e^{i\frac{\Delta}{v_s} r \sinh \theta} e^{2\frac{\Delta}{v_s} x_2 \cosh \xi} e^{-\Delta\tau \cosh \theta}. \quad (\text{C41})$$

The next term in the series (C30) is  $C_{32}$ , its disconnected piece is similar to  $C_{12}^1$  and reads explicitly

$$C_{32}^1 = -Z_1 \frac{e^{-i\frac{\pi}{4}}}{\sqrt{2}} \int_{-\infty}^{\infty} \frac{d\xi d\theta}{2\pi} \frac{K^{\sigma\bar{\sigma}}(\xi)}{\cosh \xi} \frac{i e^{\xi} + e^{\theta}}{e^{\xi+\theta} - i} e^{\xi/2} e^{i\frac{\Delta}{v_s} r \sinh \theta} e^{2\frac{\Delta}{v_s} x_1 \cosh \xi} e^{-\Delta\tau \cosh \theta}. \quad (\text{C42})$$

The terms  $C_{12}^1$  and  $C_{32}^1$  are of the same order and yield together the contribution to the LDOS denoted by  $N_{11}$ .

The term resulting in  $N_{21}$  is

$$C_{32}^2 = -\frac{Z_1}{2} e^{i\frac{\pi}{4}} \int_{-\infty}^{\infty} \frac{d\xi}{2\pi} \frac{d\theta_1 d\theta_2}{(2\pi)^2} e^{i\frac{\Delta}{v_s} r \sum_i \sinh \theta_i} e^{2i\frac{\Delta}{v_s} R \sinh \xi} e^{-\Delta\tau(\sum_i \cosh \theta_i + \cosh \xi)} \\ \times \left[ \frac{K^{\sigma\bar{\sigma}}(\xi + i\frac{\pi}{2}) e^{\xi/2} \sinh \frac{\xi - \theta_1}{2} \sinh \frac{\xi + \theta_1}{2}}{\cosh^2 \frac{\theta_1 - \theta_2}{2} \cosh \frac{\xi - \theta_2}{2} \cosh \frac{\xi + \theta_2}{2}} - \frac{i}{2} \frac{K^{\bar{\sigma}\sigma}(\xi + i\frac{\pi}{2}) e^{-\xi/2} \sinh^2 \frac{\theta_1 - \theta_2}{2}}{\prod_i \cosh \frac{\xi - \theta_i}{2} \cosh \frac{\xi + \theta_i}{2}} \right]. \quad (C43)$$

The final term we wish to evaluate is the disconnected piece of  $C_{14}$ . Considering first  $f_\sigma = -1$  and keeping in mind that we have restricted ourselves to the LEP, we can start with

$$C_{14} = \frac{1}{2} \int_{-\infty}^{\infty} \frac{d\xi_1 d\xi_2}{(2\pi)^2} \frac{d\theta}{2\pi} K^{-+}(\xi_1) K^{-+}(\xi_2) e^{\frac{\Delta}{v_s} r \cosh \theta} e^{2\frac{\Delta}{v_s} x_2 \sum_i \cosh \xi_i} e^{i\Delta\tau \sinh \theta} \\ \times \langle 0 | e^{\frac{i}{2}\phi_s} | \theta \rangle_+ + \langle \theta | e^{\frac{i}{2}\bar{\phi}_s} | -\xi_1, \xi_1, -\xi_2, \xi_2 \rangle_{-+-+}. \quad (C44)$$

In the second matrix element we keep only the disconnected piece

$$+ \langle \theta | e^{\frac{i}{2}\bar{\phi}_s} | -\xi_1, \xi_1, -\xi_2, \xi_2 \rangle_{-+-+} = 2\pi\delta(\theta - \xi_1) \langle 0 | e^{\frac{i}{2}\bar{\phi}_s} | -\xi_1, -\xi_2, \xi_2 \rangle_{--++} + 2\pi\delta(\theta - \xi_2) \langle 0 | e^{\frac{i}{2}\bar{\phi}_s} | -\xi_1, \xi_1, -\xi_2 \rangle_{-+-} + \dots \quad (C45)$$

In the resulting term  $C_{14}^0$  we can shift the contour of integration,  $\xi_1 \rightarrow \xi_1 + i\pi/2$ , to obtain

$$C_{14}^0 = -\frac{Z_1}{\sqrt{2}} e^{-i\frac{\pi}{4}} \int_{-\infty}^{\infty} \frac{d\xi_1 d\xi_2}{(2\pi)^2} K^{\sigma\bar{\sigma}}(\xi_1 + i\frac{\pi}{2}) K^{\sigma\bar{\sigma}}(\xi_2) \frac{e^{(\xi_1 + \xi_2)/2}}{\cosh \xi_2} \frac{e^{\xi_1} + ie^{\xi_2}}{e^{\xi_1 + \xi_2} - i} e^{2i\frac{\Delta}{v_s} R \sinh \xi_1} e^{2\frac{\Delta}{v_s} x_2 \cosh \xi_2} e^{-\Delta\tau \cosh \xi_1}. \quad (C46)$$

In the last step we have assumed that there exist no boundary bound states (see below). Finally, we mention that the next term,  $C_{34}^0$ , equals  $C_{14}^0$  with the coordinates  $x_1$  and  $x_2$  interchanged. These two terms together yield  $N_{02}$ .

The remaining two terms  $N_{12}$  and  $N_{03}$  discussed in Sec. IV C follow from  $C_{14}^1 + C_{34}^1 + C_{54}^1$  and  $C_{16}^0 + C_{36}^0 + C_{56}^0$  respectively.

## 5. Boundary bound states

As discussed above, general Dirichlet boundary conditions  $\Phi_s(0) = \Phi_s^0 \neq 0$  can result in the appearance of a boundary bound state. If  $K_s^2\pi < \Phi_s^0 < \pi$  the boundary reflection amplitude  $K^{-+}(\xi)$  has a pole in the physical strip  $0 \leq \Im \xi \leq \pi/2$  located at<sup>46,55</sup>  $\xi = i(\pi - \Phi_s^0)/(2 - 2K_s^2)$ . On the other hand,  $K^{+-}(\xi)$  is analytic in the physical strip but has a pole for  $-\pi/2 \leq \Im \xi \leq 0$ . We write the respective residues as

$$i \text{Res}[K^{\mp\pm}(\xi), \xi = \pm i\gamma] = B \geq 0, \quad \gamma = \frac{\pi - \Phi_s^0}{2 - 2K_s^2}, \quad (C47)$$

where  $B$  depends on  $K_s$  only. We have checked the sign of  $B$  by performing an explicit mode expansion at the LEP as well as studying the spectral function of the correlator  $\langle 0_b | e^{-ia\Phi_s'(\tau, R)} e^{ia\Phi_s'(0, R)} | 0_b \rangle$  (for which the relevant form factors were obtained in Ref. [67]).

In the presence of a boundary bound state the poles of  $K^{\mp\pm}(\xi)$  will contribute whenever we shift the contour of integration  $\xi \rightarrow \xi \pm i\pi/2$  in a given term in the form-factor expansion (C30). The leading term of this type is obtained from (C38), which yields (41) by a straightforward calculation. The sub-leading term can be obtained similarly from  $C_{14}^0$  and  $C_{34}^0$ . At the LEP it is given by ( $B = -2\cos\Phi_s^0$ ,  $\pi/2 \leq \Phi_s^0 \leq \pi$ )

$$\Theta\left(\Phi_s^0 - \frac{\pi}{2}\right) \delta_{\sigma\downarrow} Z_1 \sqrt{8} e^{-\frac{i}{2}\Phi_s^0} \cos \Phi_s^0 e^{-2\frac{\Delta}{v_s} R \cos \Phi_s^0} e^{-\Delta\tau \sin \Phi_s^0} \int_{-\infty}^{\infty} \frac{d\xi}{2\pi} \frac{K^{\sigma\bar{\sigma}}(\xi)}{\cosh \xi} \frac{\cosh\left(\frac{\xi}{2} + \frac{i}{2}\Phi_s^0\right)}{\sinh\left(\frac{\xi}{2} - \frac{i}{2}\Phi_s^0\right)} e^{\xi/2} e^{2\frac{\Delta}{v_s} x_2 \cosh \xi}. \quad (C48)$$

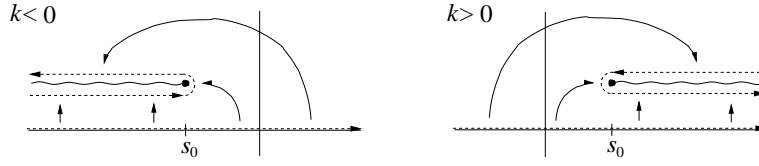


FIG. 14: Branch cut and deformation of the contour of integration used for  $k < 0$  and  $k > 0$  respectively.

#### Appendix D: Fourier transformation of the LDOS

We calculate the auxiliary function

$$I(\omega, k) = \int_{-\infty}^0 dR \int_{-\infty}^{\infty} dt \frac{e^{i(\omega t - kR)}}{(v_c \tau - 2iR)^a} \frac{1}{(v_c \tau + 2iR)^b} \left( \frac{2R}{v_c \tau} \right)^{2c} \Big|_{\tau \rightarrow it + \delta} \quad (D1)$$

$$= \int_{-\infty}^0 dR \int_{-\infty}^{\infty} dt \frac{e^{i(\omega t - kR)}}{(v_c t - 2R - i\delta)^a} \frac{(-i)^{a+b+2c}}{(v_c t + 2R - i\delta)^b} \left( \frac{2R}{v_c t - i\delta} \right)^{2c}, \quad (D2)$$

where  $v_c, a, b, c \in \mathbb{R}$ ,  $v_c > 0$ ,  $a + b < 2$  and  $c > -1/2$ . We substitute  $R \rightarrow -R$  and  $t \rightarrow -t$ , introduce  $s = v_c t/2R$  and  $\eta \rightarrow 0+$ , and perform the resulting  $R$ -integral (3.381.4 in Ref. [63]), which yields

$$I(\omega, k) = -\frac{e^{i\pi(a+b-c)} \Gamma(2-a-b)}{2^{a+b-1} v_c} \int_{-\infty}^{\infty} ds \frac{\left( \frac{2\omega}{v_c} s - k - i\eta \right)^{a+b-2}}{(s-1+i\delta)^a (s+1+i\delta)^b (s+i\delta)^{2c}}. \quad (D3)$$

For  $\omega < 0$  the integrand has all its branch points in the lower half plane and the integral over  $s$  vanishes as long as  $c > -1/2$ . Hence we find ( $s_0 = v_c k/2\omega$ )

$$I(\omega, k) = -\Theta(\omega) \Gamma(2-a-b) \frac{e^{i\pi(a+b-c)} \omega^{a+b-2}}{2 v_c^{a+b-1}} \int_{-\infty}^{\infty} ds \frac{(s - s_0 - i\eta)^{a+b-2}}{(s-1+i\delta)^a (s+1+i\delta)^b (s+i\delta)^{2c}}. \quad (D4)$$

First consider the case  $k < 0$ . The numerator of the integrand has a branch point at  $s = s_0 + i\eta$  in the upper half plane. We place the cut running from  $-\infty + i\eta$  to  $s_0 + i\eta$  with constant imaginary part (see Fig. 14). Now we deform the contour of integration and rewrite the integration above the cut as integration below the cut using

$$\int_{-\infty}^{\infty} ds (s - s_0 - i\eta)^{a+b-2} g(s) = \int_{-\infty}^{s_0} ds (s - s_0 - i\eta)^{a+b-2} g(s) \left[ 1 - e^{2\pi i(a+b)} \right]. \quad (D5)$$

Assuming  $1 < a + b$  and substituting  $s = s_0/t$  this yields for the integral in (D4)

$$-2i \sin(\pi(a+b)) |s_0|^{a+b-1} \int_0^1 dt \frac{t^{2c} (1-t)^{a+b-2}}{(s_0 - t + i\delta)^a (s_0 + t + i\delta)^b (s_0 + i\delta)^{2c}}. \quad (D6)$$

Finally, using (recall  $s_0 < 0$ ,  $\delta = 0+$ )

$$(s_0 - t + i\delta)^{-a} = (s_0(1 - (1/s_0 + i\delta)t))^{-a} = |s_0|^{-a} e^{-i\pi a} (1 - (1/s_0 + i\delta)t)^{-a} \quad (D7)$$

$$(s_0 + t + i\delta)^{-b} = (s_0(1 + (1/s_0 - i\delta)t))^{-b} = |s_0|^{-b} e^{-i\pi b} (1 + (1/s_0 - i\delta)t)^{-b} \quad (D8)$$

$$(s_0 + i\delta)^{-2c} = |s_0|^{-2c} e^{-2\pi i c}, \quad (D9)$$

as well as  $e^{-2\pi i c}/|s_0|^{2c+1} = -(1/s_0 - i\delta)^{2c+1}$  and  $\Gamma(z)\Gamma(1-z) = \pi/\sin(\pi z)$  we obtain

$$I(\omega, k < 0) = \frac{\pi \Theta(\omega) e^{-i\frac{\pi}{2}(2c-1)}}{\Gamma(a+b-1)} \frac{\omega^{a+b-2}}{v_c^{a+b-1}} \left( \frac{1}{s_0} - i\delta \right)^{2c+1} \int_0^1 dt \frac{t^{2c} (1-t)^{a+b-2}}{(1 - (1/s_0 + i\delta)t)^a (1 + (1/s_0 - i\delta)t)^b}. \quad (D10)$$

For  $k > 0$  we place the cut as shown in Fig. 14. Performing the same steps as above we find

$$I(\omega, k > 0) = \frac{\pi \Theta(\omega) e^{-i\frac{\pi}{2}(2c-1)}}{\Gamma(a+b-1)} \frac{\omega^{a+b-2}}{v_c^{a+b-1}} \left( \frac{1}{s_0} + i\delta \right)^{2c+1} \int_0^1 dt \frac{t^{2c} (1-t)^{a+b-2}}{(1 - (1/s_0 - i\delta)t)^a (1 + (1/s_0 + i\delta)t)^b}. \quad (D11)$$

We can write (D10) and (D11) together as

$$I(\omega, k) = \frac{\pi \Theta(\omega) e^{-i\frac{\pi}{2}(2c-1)} \Gamma(2c+1) \omega^{a+b-2}}{\Gamma(a+b+2c) v_c^{a+b-1}} u^{2c+1} F_1(2c+1, a, b, a+b+2c; u^*, -u), \quad u = \frac{2\omega}{v_c k} + i \operatorname{sgn}(k) \delta. \quad (\text{D12})$$

Here we have used the integral representation (E2) of Appell's hypergeometric function<sup>49</sup>, which is valid for  $1 < a+b$ . Analytic continuation in the parameters  $a$ ,  $b$ , and  $c$  then yields  $I(\omega, k)$  for  $a+b < 2$  and  $c > -1/2$ . At  $K_c = 1$  one finds  $F_1(2c+1, a, b, a+b+2c; u^*, -u) = F_1(1, 1/2, 0, 1/2; u^*, -u) = 1/(1-u^*)$ .

In the same way one can show

$$\begin{aligned} & \int_{-\infty}^0 dR \int_{-\infty}^{\infty} dt \frac{e^{i(\omega t - kR)}}{(v_c t - 2R - i\delta)^c} \frac{(-i)^{a+b+2c}}{(v_c t + 2R - i\delta)^c} \frac{(2R)^{2c}}{(v_c t - i\delta)^{a+b}} \\ &= \pi \Theta(\omega) e^{-i\frac{\pi}{2}(2c-1)} \frac{\omega^{a+b-2}}{v_c^{a+b-1}} \frac{\Gamma(a+b+1)}{\Gamma(2a+2b)} u^{2c+1} F_1(a+b+1, c, c, 2a+2b; u^*, -u), \quad u = \frac{2\omega}{v_c k} + i \operatorname{sgn}(k) \delta, \end{aligned} \quad (\text{D13})$$

as well as ( $A > 0$ )

$$\begin{aligned} & \int_{-\infty}^0 dR \int_{-\infty}^{\infty} dt \frac{e^{i(\omega t - kR)}}{(v_c t - 2R - i\delta)^a} \frac{(-i)^{a+b+2c} e^{AR}}{(v_c t + 2R - i\delta)^b} \left( \frac{2R}{v_c t - i\delta} \right)^{2c} = \frac{\pi \Theta(\omega) e^{-i\frac{\pi}{2}(2c-1)}}{\omega^{2-a-b} v_c^{a+b-1}} \frac{\Gamma(2c+1)}{\Gamma(a+b+2c)} \\ & \times \left( \frac{2\omega}{v_c k} + i \operatorname{sgn}(k) \delta \right)^{2c+1} F_D^{(3)} \left( 2c+1, a, b, 2c, a+b+2c; \frac{2\omega}{v_c k} - i\frac{A}{k}, -\frac{2\omega}{v_c k} - i\frac{A}{k}, -i\frac{A}{k} \right), \end{aligned} \quad (\text{D14})$$

where  $F_D^{(3)}$  denotes Lauricella's hypergeometric function of three variables (see App. E). For  $a = 1/2$  and  $b = c = 0$  (D14) simplifies to  $2i\sqrt{\pi v_c} \Theta(\omega) / \sqrt{\omega} / (v_c k - 2\omega + i v_c A)$ .

## Appendix E: Hypergeometric function of several variables

Hypergeometric series of several variables were first studied by Lauricella<sup>56</sup>. They are defined by

$$F_D^{(n)}(\alpha, \beta_1, \dots, \beta_n, \gamma; z_1, \dots, z_n) = \sum_{m_1, \dots, m_n=0}^{\infty} \frac{(\alpha)_{m_1+\dots+m_n} (\beta_1)_{m_1} \dots (\beta_n)_{m_n}}{(\gamma)_{m_1+\dots+m_n}} \frac{z_1^{m_1} \dots z_n^{m_n}}{m_1! \dots m_n!}, \quad |z_i| < 1. \quad (\text{E1})$$

The special cases<sup>49</sup>  $n = 1$  and  $n = 2$  are Gauss hypergeometric function  $F_D^{(1)} = F(\alpha, \beta; \gamma; z)$ , and Appell's hypergeometric function  $F_D^{(2)} = F_1(\alpha, \beta_1, \beta_2, \gamma; z_1, z_2)$ , respectively. The function  $F_D^{(n)}$  possesses the Euler-type integral representation<sup>49,68</sup>

$$F_D^{(n)}(\alpha, \beta_1, \dots, \beta_n, \gamma; z_1, \dots, z_n) = \frac{\Gamma(\gamma)}{\Gamma(\alpha) \Gamma(\gamma - \alpha)} \int_0^1 dt \frac{t^{\alpha-1} (1-t)^{\gamma-\alpha-1}}{(1-z_1 t)^{\beta_1} \dots (1-z_n t)^{\beta_n}}, \quad \Re \alpha > 0, \Re(\gamma - \alpha) > 0. \quad (\text{E2})$$

Furthermore the following relations hold<sup>49,56</sup>

$$F_D^{(n)}(\alpha, \beta_1, \dots, \beta_n, \gamma; z_1, \dots, z_n) = (1-z_1)^{-\beta_1} \dots (1-z_n)^{-\beta_n} F_D^{(n)}\left(\gamma - \alpha, \beta_1, \dots, \beta_n, \gamma; \frac{z_1}{z_1-1}, \dots, \frac{z_n}{z_n-1}\right), \quad (\text{E3})$$

$$F_1(\alpha, \beta_1, \beta_2, \gamma; 1, 1) = \frac{\Gamma(\gamma) \Gamma(\gamma - \alpha - \beta_1 - \beta_2)}{\Gamma(\gamma - \alpha) \Gamma(\gamma - \beta_1 - \beta_2)} \quad \text{for } \gamma \neq 0, -1, -2, \dots \text{ and } \gamma > \alpha + \beta_1 + \beta_2. \quad (\text{E4})$$

## Appendix F: Properties of $N_{\sigma}^>(E, 2k_F + q)$

In order to analyze the dispersing features and singularities of (26) we first note that  $F_1(2c+1, a, b, a+b+2c; u^*, -u)$  possesses singularities at  $u = \pm 1$ .

Let us first study  $N_1^>$ . The integrand has singularities at

$$(i) \quad E - \Delta \cosh \theta = 0, \quad (ii) \quad 2(E - \Delta \cosh \theta) = \pm v_c q. \quad (\text{F1})$$

Inserting (i) into (ii) immediately yields a feature at  $q = 0$ . Using (E3) and (E4) one can extract the  $q$ -dependence  $(v_c q)^{a+b-2c-1}$  to obtain (29). On the other hand, (i) will be stationary at  $\theta \approx 0$ . Inserting this into (ii) directly yields the dispersion relation (30). The suppression of the dispersing peak for  $q < 0$  follows from the relative strength of the singularities at  $u = \pm 1$ .

In the same way the integrand in  $N_2^>$  has singularities at

$$(i) \quad E - \Delta \cosh \theta = 0, \quad (iii) \quad 2v_s(E - \Delta \cosh \theta) = \pm v_c(v_s q - 2\Delta \sinh \theta). \quad (F2)$$

Inserting (i) into (iii) directly yields the dispersion relation (31). Furthermore, we can rewrite (iii) as

$$(iv) \quad \frac{E}{\Delta} \mp \frac{v_c q}{2\Delta} = \cosh \theta \mp \frac{v_c}{v_s} \sinh \theta. \quad (F3)$$

If and only if  $v_c < v_s$ , the right-hand side in (iv) becomes stationary at  $\theta = \tilde{\theta} = \pm \text{arccosh}(v_s/\sqrt{v_s^2 - v_c^2})$ . In principle, this leads to the relation (32) for arbitrary  $q$ . However, this dispersing feature only exists when  $-\text{arccosh}(\frac{E}{\Delta}) \leq \tilde{\theta} \leq \text{arccosh}(\frac{E}{\Delta})$ . Together with (32) this yields the condition  $q_0 \leq |q|$ .

Finally, in order to prove (45) we use that  $F_D^{(3)}(2c+1, a, b, 2c, a+b+2c; u_3^*, -u_3, -u_3')$  is regular as  $E \rightarrow E_{\text{bbs}}+$ , which directly yields  $\alpha = 1 - a - b - 2c = 1 - 1/(2K_c^2)$ .

- 
- <sup>1</sup> T. W. Odom, J.-L. Huang, and C. M. Lieber, *J. Phys.: Condens. Matter* **14**, R145 (2002).
  - <sup>2</sup> C. Howald, P. Fournier, and A. Kapitulnik, *Phys. Rev. B* **64**, 100504(R) (2001).
  - <sup>3</sup> J. E. Hoffman, K. McElroy, D.-H. Lee, K. M. Lang, H. Eisaki, S. Uchida, and J. C. Davis, *Science* **297**, 1148 (2002); K. McElroy, R. W. Simmonds, J. E. Hoffman, D.-H. Lee, J. Orenstein, H. Eisaki, S. Uchida, and J. C. Davis, *Nature* **422**, 592 (2003); C. Howald, H. Eisaki, N. Kaneko, M. Greven, and A. Kapitulnik, *Phys. Rev. B* **67**, 014533 (2003); M. Vershinin, S. Misra, S. Ono, Y. Abe, Y. Ando, and A. Yazdani, *Science* **303**, 1995 (2004).
  - <sup>4</sup> Y. Kohsaka, C. Taylor, K. Fujita, A. Schmidt, C. Lupien, T. Hanaguri, M. Azuma, M. Takano, H. Eisaki, H. Takagi, S. Uchida, and J. C. Davis, *Science* **315**, 1380 (2007).
  - <sup>5</sup> O. Fischer, M. Kugler, I. Maggio-Aprile, C. Berthod, and C. Renner, *Rev. Mod. Phys.* **79**, 353 (2007).
  - <sup>6</sup> A. Fang, N. Ru, I. R. Fisher, and A. Kapitulnik, *Phys. Rev. Lett.* **99**, 046401 (2007).
  - <sup>7</sup> R. Wiesendanger, H. J. Güntherrodt, G. Güntherrodt, R. J. Gambino, and R. Ruf, *Phys. Rev. Lett.* **65**, 247 (1990); R. Wiesendanger, I. V. Shvets, D. Bürgler, G. Tarrach, H. J. Güntherrodt, J. M. D. Coey, and S. Gräser, *Science* **255**, 583 (1992); S. Heinze, M. Bode, A. Kubetzka, O. Pietzsch, X. Nie, S. Blügel, and R. Wiesendanger, *Science* **288**, 1805 (2000).
  - <sup>8</sup> S. Eggert, *Phys. Rev. Lett.* **84**, 4413 (2000); P. Kakashvili, H. Johannesson, and S. Eggert, *Phys. Rev. B* **74**, 085114 (2006); I. Schneider, A. Struck, M. Bortz, and S. Eggert, *Phys. Rev. Lett.* **101**, 206401 (2008); M. Guigou, T. Martin, and A. Crepieux, *Phys. Rev. B* **80**, 045420 (2009); I. Schneider and S. Eggert, *Phys. Rev. Lett.* **104**, 036402 (2010).
  - <sup>9</sup> S. A. Kivelson, I. P. Bindloss, E. Fradkin, V. Oganessian, J. M. Tranquada, A. Kapitulnik, and C. Howald, *Rev. Mod. Phys.* **75**, 1201 (2003).
  - <sup>10</sup> A. Polkovnikov, M. Vojta, and S. Sachdev, *Phys. Rev. B* **65**, 220509 (2002); Q.-H. Wang and D.-H. Lee, *Phys. Rev. B* **67**, 020511 (2003).
  - <sup>11</sup> D. Podolsky, E. Demler, K. Damle, and B. I. Halperin, *Phys. Rev. B* **67**, 094514 (2003).
  - <sup>12</sup> C. L. Kane and M. P. A. Fisher, *Phys. Rev. Lett.* **68**, 1220 (1992); C. L. Kane and M. P. A. Fisher, *Phys. Rev. B* **46**, 15233 (1992).
  - <sup>13</sup> M. Grioni, S. Pons, and E. Frantzeskakis, *J. Phys.: Condens. Matter* **21**, 023201 (2009) and references therein.
  - <sup>14</sup> C. Bourbonnais and D. Jerome, in *Advances in Synthetic Metals, Twenty years of Progress in Science and Technology*, edited by P. Bernier, S. Lefrant, and G. Bidan (Elsevier, New York, 199), p. 206; T. Giamarchi, *Chem. Reviews* **104**, 5037 (2004) and references therein; A. Schwartz, M. Dressel, G. Grüner, V. Vescoli, L. Degiorgi, and T. Giamarchi, *Phys. Rev. B* **58**, 1261 (1998).
  - <sup>15</sup> I. A. Zaliznyak, H. Woo, T. G. Perring, C. L. Broholm, C. D. Frost, and H. Takagi, *Phys. Rev. Lett.* **93**, 087202 (2004); B. J. Kim, H. Koh, E. Rotenberg, S.-J. Oh, H. Eisaki, N. Motoyama, S. Uchida, T. Tohyama, S. Mackawa, Z.-X. Shen, and C. Kim, *Nat. Phys.* **2**, 397 (2006); T. E. Kidd, T. Valla, P. D. Johnson, K. W. Kim, G. D. Gu, and C. C. Homes, *Phys. Rev. B* **77**, 054503 (2008).
  - <sup>16</sup> J. W. G. Wildöer, L. C. Venema, A. G. Rinzier, R. E. Smalley, and C. Dekker, *Nature* **391**, 59 (1998); L. C. Venema, J. W. Janssen, M. R. Buitelaar, J. W. G. Wildöer, S. G. Lemay, L. P. Kouwenhoven, and C. Dekker, *Phys. Rev. B* **62**, 5238 (2000); P. M. Singer, P. Wzietek, H. Alloul, F. Simon, and H. Kuzmany, *Phys. Rev. Lett.* **95**, 236403 (2005).
  - <sup>17</sup> S. Notbohm, P. Ribeiro, B. Lake, D. A. Tennant, K. P. Schmidt, G. S. Uhrig, C. Hess, R. Klingeler, G. Behr, B. Büchner, M. Reehuis, R. I. Bewley, C. D. Frost, P. Manuel, and R. S. Eccleston, *Phys. Rev. Lett.* **98**, 027403 (2007).
  - <sup>18</sup> P. Chudzinski, M. Gabay, and T. Giamarchi, *New J. Phys.* **11**, 055059 (2009).
  - <sup>19</sup> E. Arrigoni, E. Fradkin, and S. A. Kivelson, *Phys. Rev. B* **69**, 214519 (2004); E. W. Carlson, V. J. Emery, S. A. Kivelson, and D. Orgad, in *The Physics of Superconductors*, edited by K. H. Bennemann and J. B. Ketterson (Springer, Berlin, 2004), Vol. II; R. M. Konik, F. H. L. Essler, and A. M. Tsvelik, *Phys. Rev. B* **78**, 214509 (2008).



- <sup>20</sup> D. Schuricht, F. H. L. Essler, A. Jaefari, and E. Fradkin, Phys. Rev. Lett. **101**, 086403 (2008).
- <sup>21</sup> P. K. Mitter and P. H. Weisz, Phys. Rev. D **8**, 4410 (1973); D. Gross and A. Neveu, Phys. Rev. D **10**, 3235 (1974); R. Dashen and Y. Frishman, Phys. Rev. D **11**, 2781 (1975).
- <sup>22</sup> F. H. L. Essler, H. Frahm, F. Göhmann, A. Klümper, and V. E. Korepin, *The One-Dimensional Hubbard Model* (Cambridge University Press, Cambridge, 2005).
- <sup>23</sup> T. Holstein, Ann. Phys. **8**, 325 (1959).
- <sup>24</sup> A. J. Heeger, S. Kivelson, J. R. Schrieffer, and W.-P. Su, Rev. Mod. Phys. **60**, 781 (1988).
- <sup>25</sup> E. Fradkin and J. E. Hirsch, Phys. Rev. B **27**, 1680 (1983).
- <sup>26</sup> In Ref. [25] only the half-filled case was discussed. At half-filling, the CDW is commensurate and, due to the existence of an Umklapp operator, the CDW does not slide. The effective field theory is a non-chiral SU(2) Gross-Neveu model. In this regime the system is effectively a Mott insulator. Away from half-filling the CDW slides as the Umklapp operator is absent (irrelevant), and the effective field theory is a chiral SU(2) Gross-Neveu model which is equivalent to a U(1) Thirring model with two flavors. This model has a continuous chiral symmetry, a consequence of the sliding invariance of the CDW. This is, in fact, the generic description of the low-energy physics of a 1D system with a CDW ground state, regardless the microscopic origin of this state.
- <sup>27</sup> S. White, I. Affleck, and D. J. Scalapino, Phys. Rev. B **65**, 165122 (2002).
- <sup>28</sup> A. M. Tsvelik, Phys. Rev. B **77**, 073402 (2008).
- <sup>29</sup> S. Ghoshal and A. B. Zamolodchikov, Int. J. Mod. Phys. A **9**, 3841 (1994); *ibid.* **9**, E4353 (1994).
- <sup>30</sup> A. MacIntyre, J. Phys. A: Math. Gen. **28**, 1089 (1995); H. Saleur, S. Skorik, and N. P. Warner, Nucl. Phys. B **441**, 421 (1995).
- <sup>31</sup> A. Luther and V. J. Emery, Phys. Rev. Lett. **33**, 589 (1974); P. A. Lee, Phys. Rev. Lett. **34**, 1247 (1975).
- <sup>32</sup> A. B. Zamolodchikov, Commun. Math. Phys. **55**, 183 (1977).
- <sup>33</sup> S. Ghoshal, Int. J. Mod. Phys. A **9**, 4801 (1994).
- <sup>34</sup> S. R. White, R. M. Noack, and D. J. Scalapino, Phys. Rev. Lett. **73**, 886 (1994); L. Balents and M. P. A. Fisher, Phys. Rev. B **53**, 12133 (1996); H.-H. Lin, L. Balents, and M. P. A. Fisher, Phys. Rev. B **56**, 6569 (1997); C. Wu, W. V. Liu, and E. Fradkin, Phys. Rev. B **68**, 115104 (2003); D. Controzzi and A. M. Tsvelik, Phys. Rev. B **72**, 035110 (2005); A. M. Tsvelik, arXiv:1004.5092.
- <sup>35</sup> H.-H. Lin, L. Balents, and M. P. A. Fisher, Phys. Rev. B **58**, 1794 (1998); R. M. Konik and A. W. W. Ludwig, Phys. Rev. B **64**, 155112 (2001); F. H. L. Essler and R. M. Konik, Phys. Rev. B **75**, 144403 (2007).
- <sup>36</sup> M. Fabrizio and A. O. Gogolin, Phys. Rev. B **51**, 17827 (1995); S. Eggert, H. Johannesson, and A. Mattsson, Phys. Rev. Lett. **76**, 1505 (1996); S. Eggert, A. E. Mattsson, and J. M. Kinaret, Phys. Rev. B **56**, R15537 (1997); A. E. Mattsson, S. Eggert, and H. Johannesson, Phys. Rev. B **56**, 15615 (1997); P. Lecheminant and E. Orignac, Phys. Rev. B **65**, 174406 (2002).
- <sup>37</sup> J. L. Cardy, Nucl. Phys. B **240**, 514 (1984); J. L. Cardy, in *Phase transitions and critical phenomena*, edited by C. Domb and J. L. Lebowitz (Academic Press, London, 1987), Vol. 11.
- <sup>38</sup> P. Di Francesco, P. Mathieu, and D. Sénéchal, *Conformal Field Theory* (Springer, New York, 1997).
- <sup>39</sup> F. A. Smirnov, *Form factors in completely integrable models of quantum field theory* (World Scientific, Singapore, 1992).
- <sup>40</sup> A. Fring, G. Mussardo, and P. Simonetti, Nucl. Phys. B **393**, 413 (1993); S. Lukyanov, Mod. Phys. Lett. A **12**, 2543 (1997); H. Babujian, A. Fring, M. Karowski, and A. Zapletal, Nucl. Phys. B **538**, 535 (1999); H. Babujian and M. Karowski, Nucl. Phys. B **620**, 407 (2002); H. Babujian and M. Karowski, J. Phys. A: Math. Gen. **35**, 9081 (2002).
- <sup>41</sup> S. Lukyanov, Commun. Math. Phys. **167**, 183 (1995).
- <sup>42</sup> S. Lukyanov and A. B. Zamolodchikov, Nucl. Phys. B **607**, 437 (2001).
- <sup>43</sup> G. Delfino, J. Phys. A: Math. Gen. **37**, R45 (2004).
- <sup>44</sup> F. H. L. Essler and R. M. Konik, in *From fields to strings: Circumnavigating theoretical physics (Ian Kogan Memorial Collection)*, edited by M. Shifman, A. Vainshtein, and J. Wheeler (World Scientific, Singapore, 2005), Vol. I.
- <sup>45</sup> M. Ameduri, R. Konik, and A. LeClair, Phys. Lett. B **354**, 376 (1995); L. Mezincescu and R. I. Nepomechie, Int. J. Mod. Phys. A **13**, 2747 (1998).
- <sup>46</sup> P. Mattsson and P. Dorey, J. Phys. A: Math. Gen. **33**, 9065 (2000).
- <sup>47</sup> J.-S. Caux, H. Saleur, and F. Siano, Nucl. Phys. B **672**, 411 (2003).
- <sup>48</sup> D. Schuricht and F. H. L. Essler, J. Stat. Mech: Theor. Exp. P11004 (2007).
- <sup>49</sup> *Higher Transcendental Functions*, edited by A. Erdélyi (McGraw-Hill, New York, 1953), Vol. I.
- <sup>50</sup> J. Voit, Eur. Phys. J. B **5**, 505 (1998); F. H. L. Essler and A. M. Tsvelik, Phys. Rev. B **65**, 115117 (2002); H. Benthien, F. Gebhard and E. Jeckelmann, Phys. Rev. Lett. **92**, 256401 (2004); T. Ulbricht and P. Schmitteckert, Eur. Phys. Lett. **89**, 47001 (2010).
- <sup>51</sup> F. H. L. Essler and A. M. Tsvelik, Phys. Rev. Lett. **90**, 126401 (2003).
- <sup>52</sup> V. P. Yurov and A. B. Zamolodchikov, Int. J. Mod. Phys. **6**, 3819 (1991).
- <sup>53</sup> J. L. Cardy and G. Mussardo, Nucl. Phys. B **410**, 451 (1993); G. Delfino and G. Mussardo, Nucl. Phys. B **455**, 724 (1995); G. Delfino and J. L. Cardy, Nucl. Phys. B **519**, 551 (1998); D. Controzzi, F. H. L. Essler, and A. M. Tsvelik, Phys. Rev. Lett. **86**, 680 (2001).
- <sup>54</sup> A. Kapustin and S. Skorik, J. Phys. A: Math. Gen. **29**, 1629 (1996); F. H. L. Essler and H. Frahm, Phys. Rev. B **56**, 6631 (1997).
- <sup>55</sup> S. Skorik and H. Saleur, J. Phys. A: Math. Gen. **28**, 6605 (1995).
- <sup>56</sup> G. Lauricella, Rend. Circ. Matem. Palermo **7**, 111 (1893).
- <sup>57</sup> F. H. L. Essler and R. M. Konik, Phys. Rev. B **78**, 100403(R) (2008); F. H. L. Essler and R. M. Konik, J. Stat. Mech.

- P09018 (2009).
- <sup>58</sup> H. W. J. Blöte, J. L. Cardy, and M. P. Nightingale, Phys. Rev. Lett. **56**, 742 (1986); I. Affleck, Phys. Rev. Lett. **56**, 746 (1986).
  - <sup>59</sup> P. Abbamonte, G. Blumberg, A. Rusydi, A. Gozar, P. G. Evans, T. Siegrist, L. Venema, H. Eisaki, E. D. Isaacs, and G. A. Sawatzky, Nature **431**, 1078 (2004).
  - <sup>60</sup> K. Magishi, S. Matsumoto, Y. Kitaoka, K. Ishida, K. Asayama, M. Uehara, T. Nagata, and J. Alimitsu, Phys. Rev. B **57**, 11533 (1998).
  - <sup>61</sup> C. V. Parker, P. Aynajian, E. H. da Silva Neto, A. Pushp, S. Ono, J. Wen, Z. Xu, G. Gu, and A. Yazdani, *Appearance of Fluctuating Stripes with the Onset of the Pseudogap Phase in the High Temperature Superconductor  $\text{Bi}_2\text{Sr}_2\text{CaCu}_2\text{O}_{8+\delta}$* , unpublished (2010) and private communication.
  - <sup>62</sup> A. O. Gogolin, A. A. Nersisyan, and A. M. Tsvelik, *Bosonization and Strongly Correlated Systems* (Cambridge University Press, Cambridge, 1998).
  - <sup>63</sup> I. S. Gradshteyn and I. M. Ryzhik, *Table of Integrals, Series, and Products* (Academic Press, London, 1980).
  - <sup>64</sup> Al. B. Zamolodchikov, Int. J. Mod. Phys. A **10**, 1125 (1995).
  - <sup>65</sup> A. B. Zamolodchikov and Al. B. Zamolodchikov, Ann. Phys. **120**, 253 (1979); L. D. Faddeev, Sov. Sci. Rev. Math. Phys. C **1**, 107 (1980).
  - <sup>66</sup> V. E. Korepin, Theor. Math. Phys. **41**, 169 (1979).
  - <sup>67</sup> S. Lukyanov, Mod. Phys. Lett. A **12**, 2543 (1997).
  - <sup>68</sup> H. Exton, *Handbook of Hypergeometric Integrals: Theory, Applications, Tables, Computer Programs* (Ellis Horwood, Chichester, 1978).